AD NUMBER

AD801723

LIMITATION CHANGES

TO:

Approved for public release; distribution is unlimited.

FROM:

**Distribution authorized to U.S. Gov't. agencies and their contractors;
Administrative/Operational Use; OCT 1949. Other requests shall be referred to Ballistic Research Laboratories, Aberdeen Proving Ground, MD 21005.**

AUTHORITY

ARL ltr dtd 21 Jul 1999

BALLISTIC RESEARCH LABORATORIES

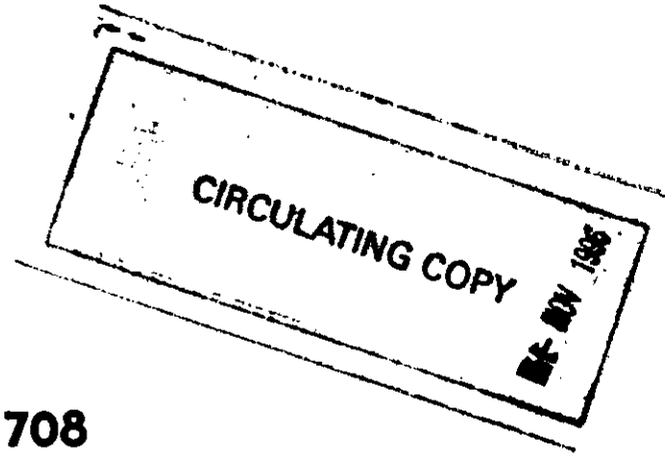

REPORT NO. 708

Optical Studies of the Jet Flame of the V-2 Missile in Flight

J. B. EDSON

ABERDEEN PROVING GROUND, MARYLAND

BALLISTIC RESEARCH LABORATORIES

REPORT NO. 708

Optical Studies of the Jet Flame of the V-2 Missile in Flight

J. B. EDSON

PROJECT NO. TB3-0538B OF THE RESEARCH AND DEVELOPMENT DIVISION, ORDNANCE DEPARTMENT

OCTOBER 1949

ABERDEEN PROVING GROUND, MARYLAND

BALLISTIC RESEARCH LABORATORIES
REPORT NO. 708

J. B. Edson
Aberdeen Proving Ground, Md.
1 August 1949

OPTICAL STUDIES OF THE JET FLAME OF THE V2 MISSILE IN FLIGHT

ABSTRACT

Generation of thrust by burning of fuel outside the missile is among the jet phenomena found in this study of the flying V2 rocket. Other items are the explanation of an abrupt change in jet structure at sonic missile velocity and a "fishtail" jet form at supersonic missile velocities.

Photometry of motion picture spectrograms has yielded the change in intensity of jet emissions as the missile rises. It appears that at higher missile velocities and altitudes the jet may not be as faint as simple theory predicts.

The motion pictures of jet details and the jet cinespectrograms were made during V2 missile firings at White Sands Proving Ground. They were obtained with the aid of tracking telescopes developed by the Ballistic Research Laboratories for detailed observation of missiles in flight at high altitudes.

OPTICAL STUDIES OF THE JET FLAME OF THE V2 MISSILE IN FLIGHT

I. INTRODUCTION

The development of tracking telescopes by the Ballistic Research Laboratories at Aberdeen Proving Ground permitted for the first time the telephotography in some detail of missiles flying at high atltitudes. Examination of motion picture records obtained with tracking telescopes at White Sands Proving Ground has led to the discovery of unforseen phenomena in the jet structure of the V2 missile.

The unexpected nature of the changes invited an attempt to understand them in terms of physical principles. There also arose the question of possible effects on missile performance. These considerations led to the collaboration of the Ballistic Research Laboratories and the Physics Department of Johns Hopkins University in a spectrographic and photographic investigation of the jet flame of the V2 missile in flight.

Some of the results and conclusions of this investigation are:

1. Spectrography of the jet flame shows that nearly all of the emitted light comes from impurities. Some of these are sodium, potassium, lithium, barium, magnesium oxide, strontium oxide, and various calcium compounds. Emission from substances found in the burning of alcohol with oxygen, specifically C_2, CO, CH, and OH, are apparently much weaker than those due to impurities. They have not been identified on any of our spectrograms to date. Conditions for spectrographic observations in the near ultraviolet have not been favorable so far.

As the missile rises, all of the flame emissions decrease in intensity in about the same proportion. This uniform behavior for various substances agrees with the flame emission theory herein set forth.

2. Comparison of measured jet cross section with spectrophotometrically determined jet temperatures thru adiabatic relationships leads to the following results:

(a) The measured jet cross section agrees with the assumption of adiabatic expansion and jet pressure equal to ambient atmospheric pressure up to about 50,000 ft. altitude.

(b) Above 50,000 ft. the jet cross section is smaller than "ambient pressure-adiabatic" assumptions require. Either the pressure on the jet surface is greater than the free air stream pressure, or the pressure fall in the jet is greater than adiabatic.

(c) Spectrophotometric jet temperatures are higher than those calculated on the "atmospheric- adiabatic" assumption. This is qualitatively consistent with (b) above and suggests that the pressure on the jet surface is greater than the free air pressure.

(d) Comparison of spectrophotometric temperatures with measured jet diameters with the aid of adiabatic relationships and assumed constant axial jet velocity leads to a ratio of specific heats $K = 1.10$ for the jet gases. This differs considerably from $K = 1.24$, the expected value as estimated from the known specific heats of the component flame gases. This suggests either that part of the jet emission may be non-thermal or that the jet gases may contain a hitherto unsuspected source of heat.

3. It is shown that for any vehicle propelled by a supersonic jet, the Mach node structure of the jet will vanish as the vehicle itself achieves supersonic velocity.

4. The delivery of a total of about four pounds per second of turbine exhaust gas thru two diametrically opposite exhaust ports into the boundary layer around the boat-tail of the V2 missile is found to have the following effects at supersonic missile velocities.

(a) Creation of a strong bilaterally symmetric pattern in the jet flame.

(b) Partly by adding low velocity material to the boundary layer and partly by burning of turbine exhaust oxygen with alcohol in the jet surface, to thicken the boundary layer around the boat-tail and thus decrease missile drag.

(c) During the later part of burning, to cause the air stream around boat-tail of the missile in the plane of the steam exhausts to diverge due to a plugging action by the burning of turbine exhaust oxygen with the alcohol in the jet flame surface at the point of "collision" between the jet surface and the air stream. This appears to be an accidental example of a novel method of creating thrust on the missile by addition of heat to the gas flow several feet away from the missile. In view of difficulties which occur with very high energy fuels, it is probably worth while to further investigate this method, in which the burning is not in contact with the rocket.

(d) It is found that the air-flame interface of a conically expanding supersonic jet flying axially in a supersonic air stream may be unstable and tend to assume an oval shape at downstream points. It is also noted that "flying wing" shapes rather than cylindrical bodies may be preferable in some types of supersonic vehicles.

II. APPEARANCE OF THE A4 JET FLAME

A. At Subsonic Missile Velocities

Until the missile reaches the speed of sound, the jet structure consists of the familiar train of "Mach nodes". In addition moving bright regions have been detected. Occasionally lateral tracking errors blur the jet image in a direction normal to the jet axis. Such images present a diagonal, "barber pole" pattern. The spiral pattern appears superposed on the streaks due to the stationary shock nodes. The diagonal streaks are apparently made by bright disturbances moving down the jet. At missile velocities much below the speed of sound, these travelling 'waves' appear at two frequencies, of approximately 70 and 140 cycles per second. Near the nozzle, the 'wave' length between brightenings is about 10 feet for the 70 and 140 cycle components alike. The velocity increases from about 700 and 1400 ft/sec. for the 70 and 140 cycle components respectively near the nozzle, to about twice those values near the tail of the jet.

The two frequencies correspond approximately to the fundamental and first harmonic of the rocket fuel pump rotation frequency.

B. At Transonic Missile Velocity

Within about a second of the passage of the missile thru sonic velocity, the Mach nodes fade and vanish. They are replaced by a different type of jet structure. Plate 1 consists of photographs selected from the 35mm motion picture record made with a tracking telescope. The slant range from telescope to missile at that time was about 9 miles. These photographs were specially printed to bring out details of the jet structure and show the passage of the jet thru sonic transition. The Mach nodes fade out, one by one, beginning at the tail of the jet. In about a second they are all gone, to be replaced by the new supersonic pattern. This same change is exhibited by every V2 missile, and may in fact be used as a dependable check upon the synchronization of film records from various tracking telescopes.

C. At Supersonic Missile Velocities

As the missile continues to gain speed and altitude the jet flame grows in diameter and assumes a flattened, fishtail appearance. The sequence of tracking telescope photographs in Plate 2 shows the typical

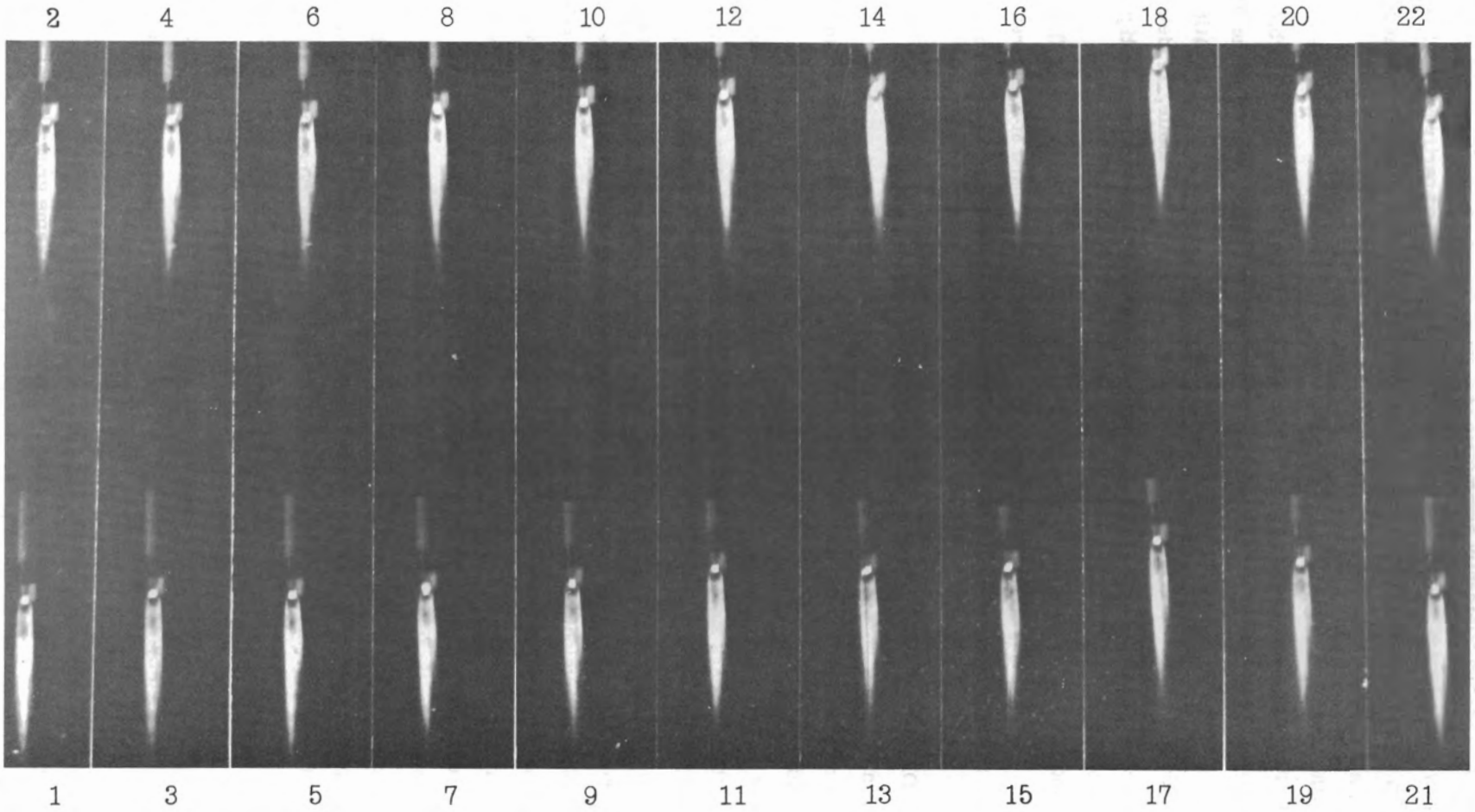

Numbers indicate frame sequence; 16 frames/sec.

Plate 1. Sonic Transition; V2 Rocket

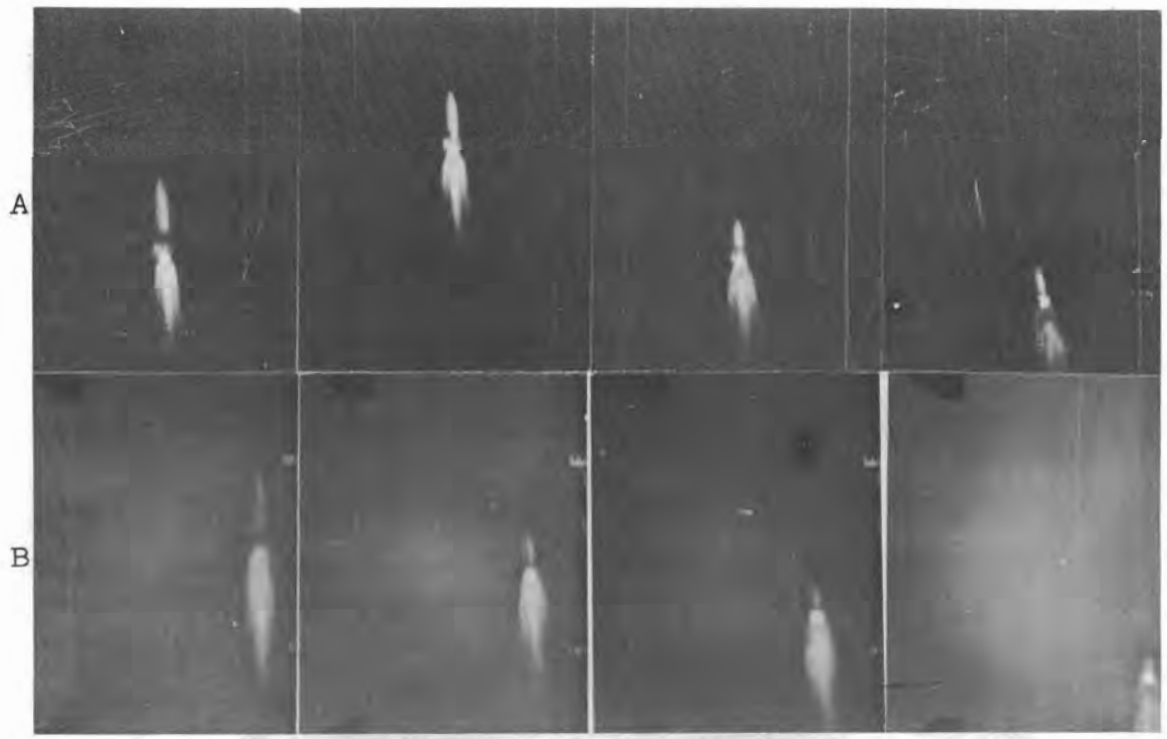

Plate 2. V2 Round 27

pattern and sequence of change, with views of the 'broad' and 'narrow' appearing aspects of the flame. Plate 3 shows a rocket which rotated. The jet rotated with it clearly displaying the flattened appearance of the flame. The rotation rates of rocket body and jet pattern are the same within the accuracy of measurement.

The jet brightness falls steadily as the missile rises. At about 55 seconds after takeoff it becomes so faint that photometry is difficult.

III. SPECTROGRAPHY OF THE JET

A. Tracking Telescopes

The two tracking telescopes employed for spectrography of the jet are known by the designations T1 and T2.

Telescope T1 consists of two 4 1/2" astronomical refractors and one pair of 20 X binoculars mounted on a modified Mount, Machine Gun Multiple, M45. This mount is electrically powered and is controlled by a pair of handlebars. The tracker sits between the telescopes and watches the missile thru the binoculars.

Telescope T2 is a 10 inch Newtonian reflecting telescope carried on the same type of mount as desscribed above for T1.

Plates 4 and 5 are photographs of T1 and T2 respectively.

B. Slitless Spectrographs

To determine the geometric distribution of intensity of various emission lines in the jet, "slitless spectrographs" were employed. For those used on Tracking Telescopes 1 and 2, the dispersion element consisted of a 1440 line/inch Wood transmission replica grating combined with a glass prism to give an undeviated ray in the green. The grating was so ruled as to concentrate intensity in one first order. This

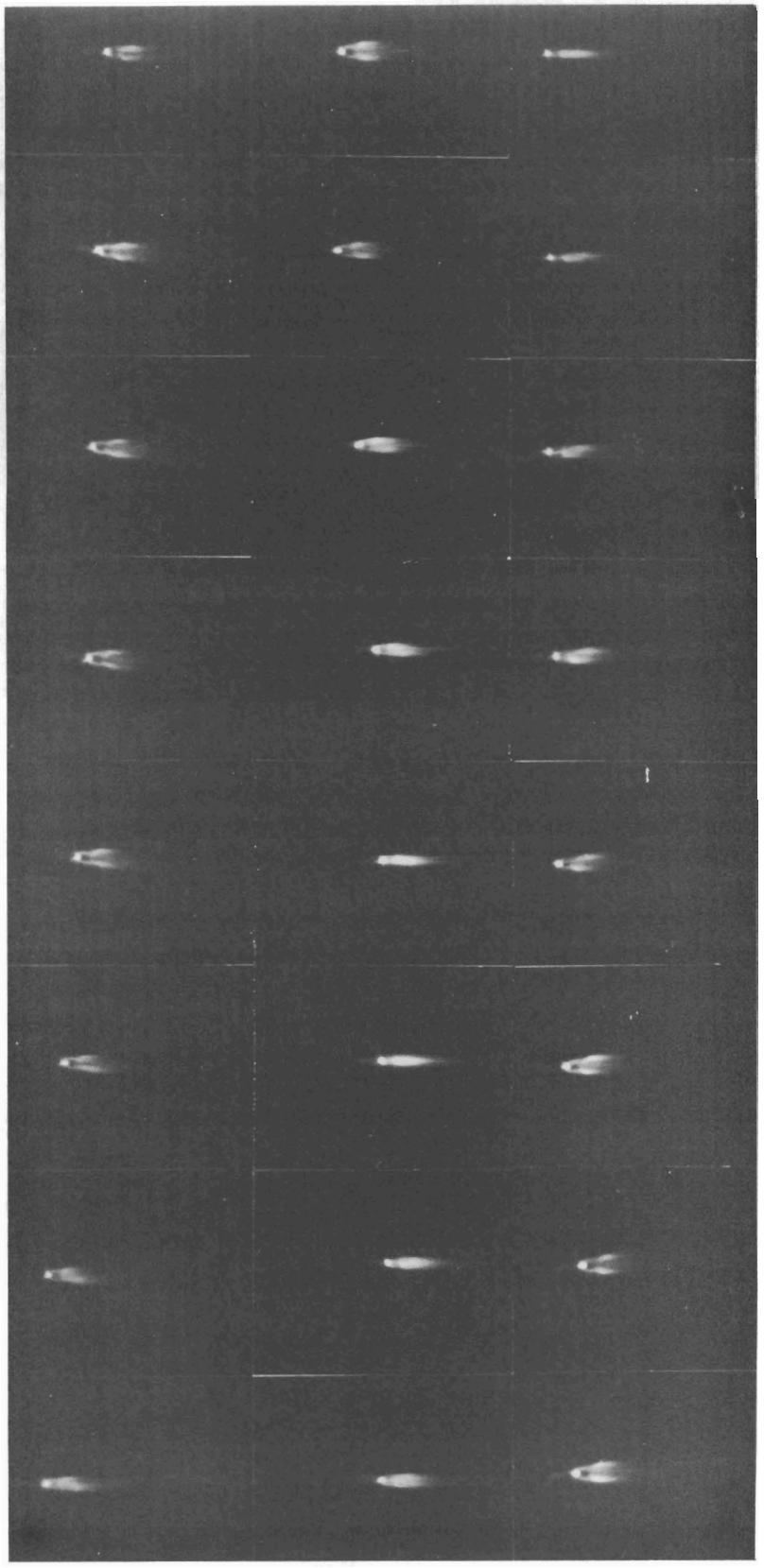

Plate 3. V2 Rocket That Rotated

16 frames/sec.

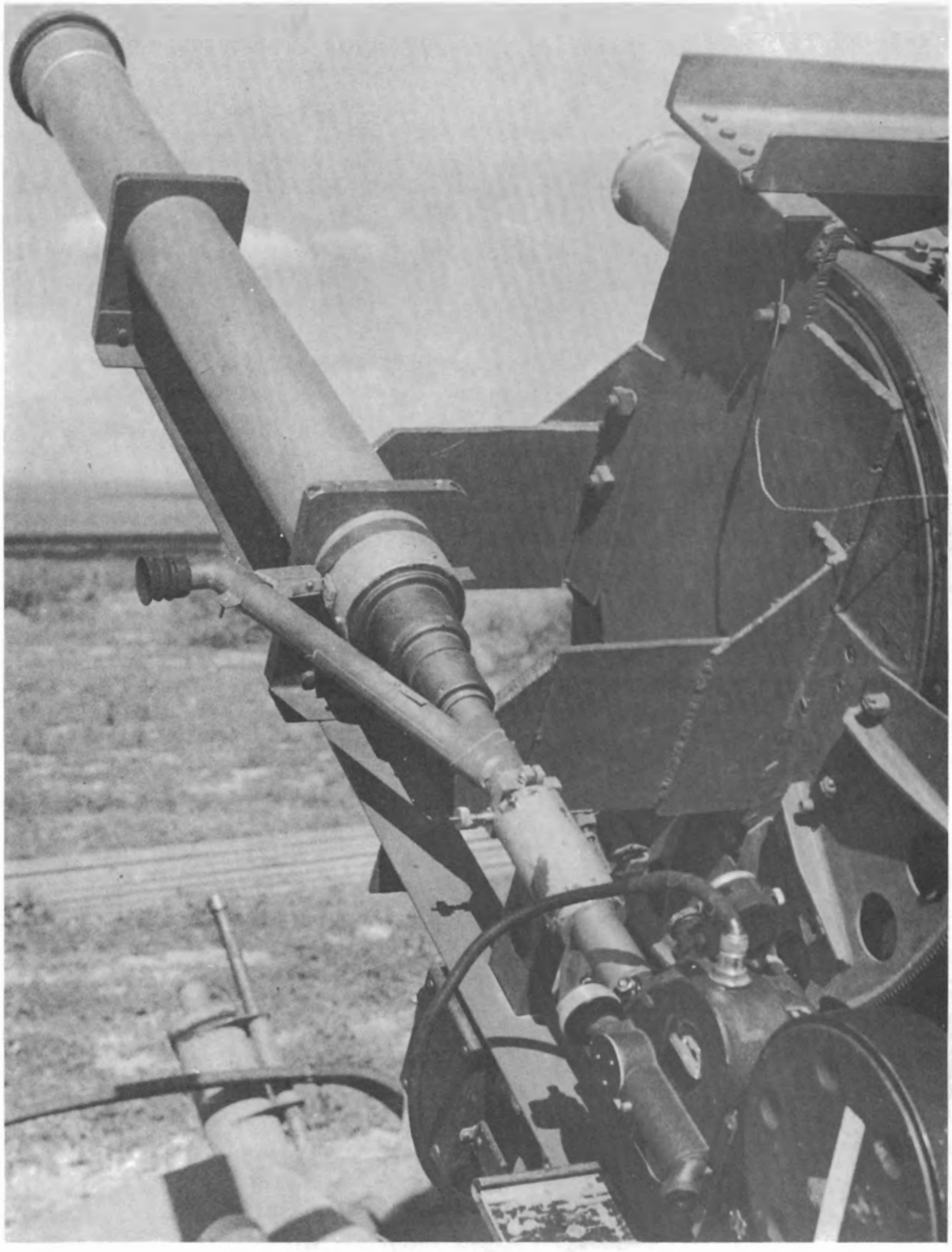

Plate 4.

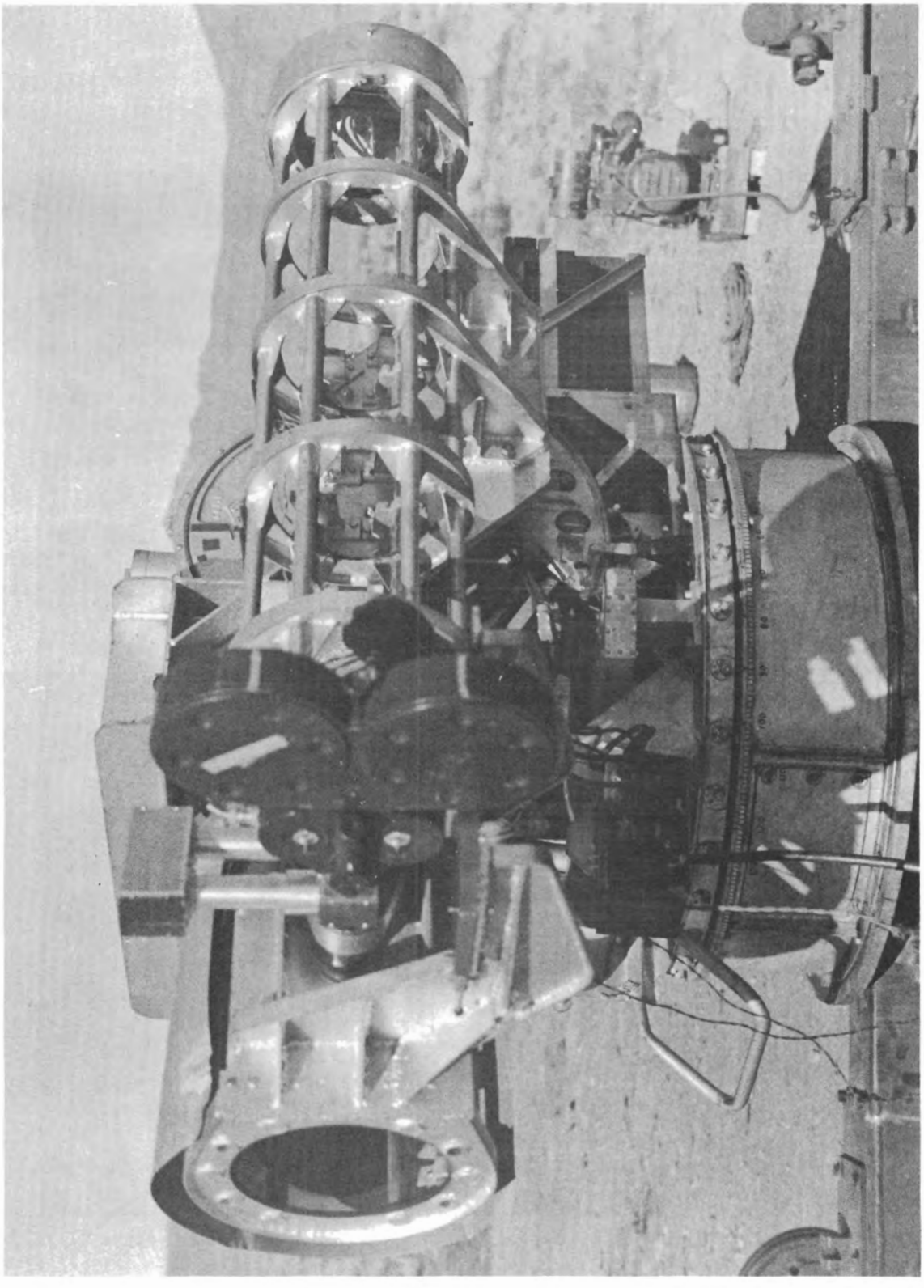

Plate 5. Interlacer on 10" Tracking Telescope

arrangement permits the conversion of the telescope into a spectrograph simply by inserting the dispersion element directly behind the amplifying lens and making a slight focal adjustment. It was used on the 4.5 inch refractor on the left side of Tracking Telescope 1.

In the case of the 10 inch reflector of Tracking Telescope 2 it was necessary to get spectra while still providing a record of direct photographs with the same telescope. To accomplish this, a device called an 'interlacer' was constructed. The interlacer produces direct photographs and spectrograms alternately on successive frames of the 35mm film record. The film is driven by a synchronous motor at the rate of 8 frames/second. In this device, the grating-prism dispersing unit is mounted on a moving carriage. During the interval when the camera shutter is closed, the disperser is carried into or out of the beam. When the shutter is open, the disperser is stationary. Plate 5 shows this device attached to the telescope.

To provide a spectrographic record including the zero order and a linear dispersion scale, a Mitchell cinetheodolite with a 12 inch focus objective was equipped with a Wood 1440 line/inch replica transmission grating. This gives approximate wave lengths for the observed flame emissions, aiding the identification of the emissions on the tracking telescope spectra. Examples of slitless spectrograms obtained with these instruments, together with identification of the observed emissions are shown in Plates 6 and 7.

Strontium nitrate was added to the fuel of Round 27, and the resulting spectrum is shown in Plate 7. This spectrum shows the red bands typical of strontium nitrate burned in air. The strong, red light of these bands makes strontium nitrate useful in flares and fireworks. Reference to the literature showed (5) (6) that the molecular source of those red 'strontium bands' was in doubt. The introduction of metallic strontium and its salts into a carbon arc in a helium atmosphere, then doing the same in an air atmosphere showed that the band source is SrO, not Sr_2. The spectra obtained are shown in Plate 8. The same results were obtained independently a few months earlier with the use of a nitrogen atmosphere at Picatinny Arsenal (7). The SrO bands, photographed under high dispersion at Johns Hopkins University, proved to be confused and complicated in structure. No detailed analysis of them is undertaken.

C. Blockhouse Spectrographs

In order to achieve a higher resolution and longer exposure than those obtained with the slitless spectrograms of the flying missile, a slit spectrograph was constructed from available parts. It was erected on the roof of the blockhouse about 200 feet from the missile launching site. The optical system consisted of a 100 cm. focus, 6" aperature Askania reflector-type objective provided with a Wood 1440 line/inch replica transmission objective grating and attached to the body of a K24 Aerial Camera. It was focused on a step slit 42 feet from the objective, and lined up so that the flame would pass thru the optic axis at a height of about 50 feet above the ground. The dispersion was about 143 Angstroms/mm. Stray light was excluded by a tube made of ventilator duct, extending from the slit to the camera. The shutter was electrically controlled from a station at one of the periscopes in the blockhouse. The exposure time was about one second, the interval required for the jet to pass along the slit. Plates 9, 10 and 11 are photographs of this instrument. Plates 12 and 13 are spectra obtained with this device, together with identification of flame emissions. Plate 12 was made at a predawn firing and is free of solar background. To facilitate identification of the flame bands observed with the blockhouse spectrograph, a sample of the well water normally used to dilute this alcohol in the A4 fuel (which is 25% water) was boiled down, acidulated slightly to hold the impurities in solution, and atomized into an acetylene flame. The resulting spectra, obtained with a 3 meter concave grating spectro-

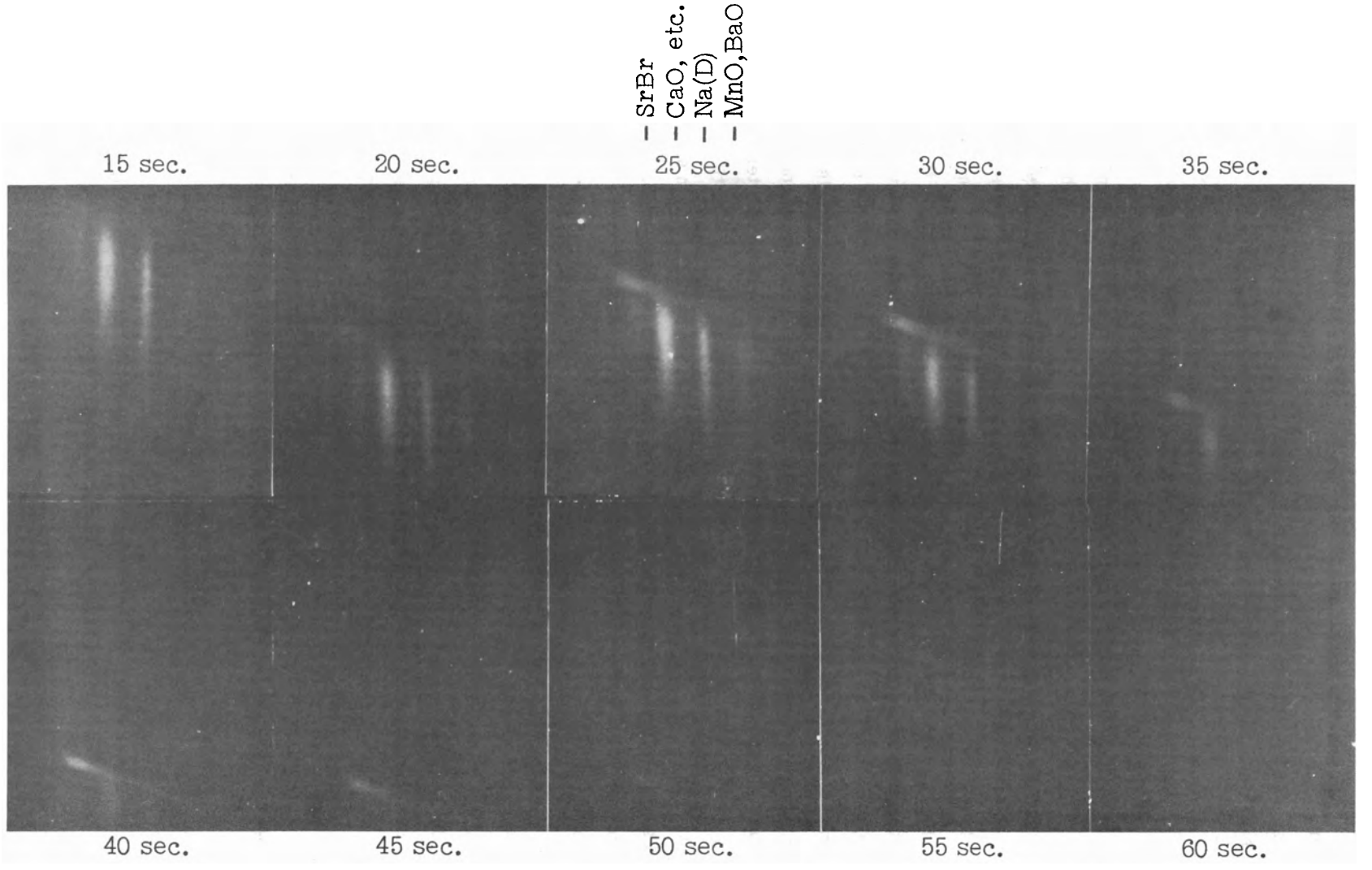

Plate 6. Slitless Spectrograms V2 Jet Without Added Substances

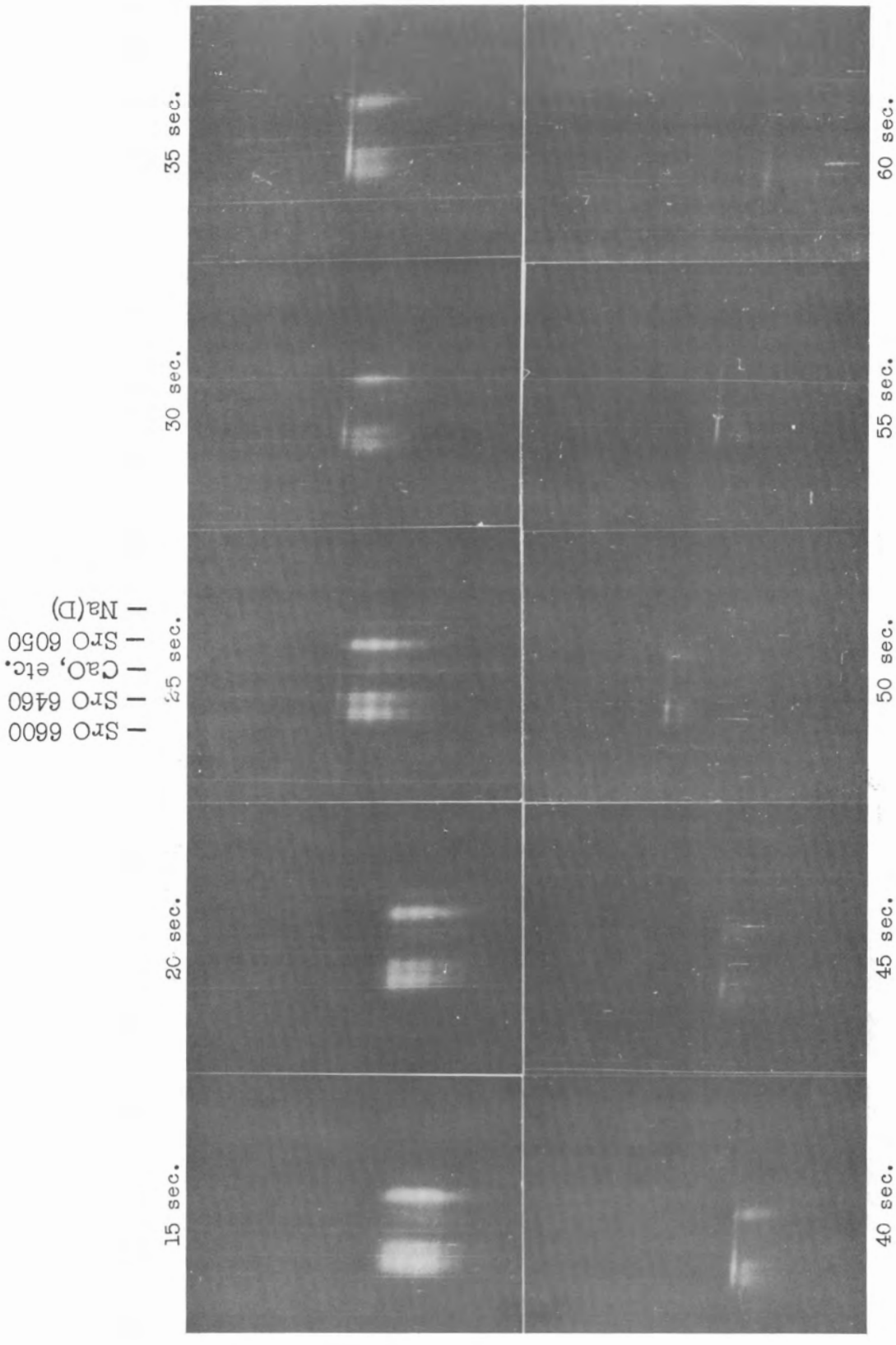

Plate 7. Slitless Spectra of V2 Round 27 showing SrO emissions

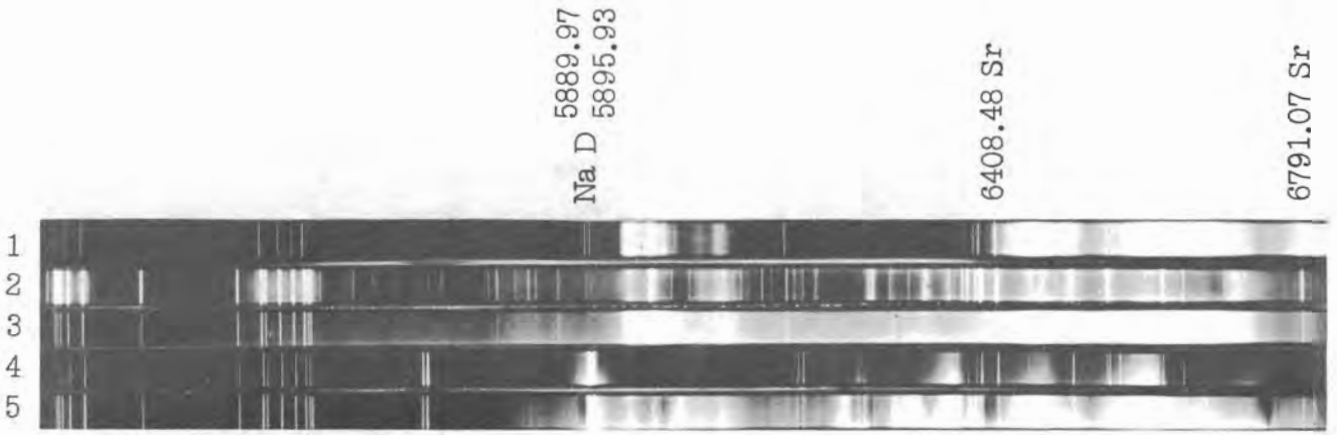

Plate 8. Carbon Arc Spectra

1. Strontium Nitrate in Air
2. Strontium Metal with slight Oxide contamination, in Helium
3. Strontium Metal with heavy Oxide coating, in Air
4. Strontium Chloride in Helium; shows chloride bands only
5. Strontium Chloride in Air

The above spectra show that the typical orange-red bands of strontium-bearing substances are due to strontium oxide, not Sr_2.

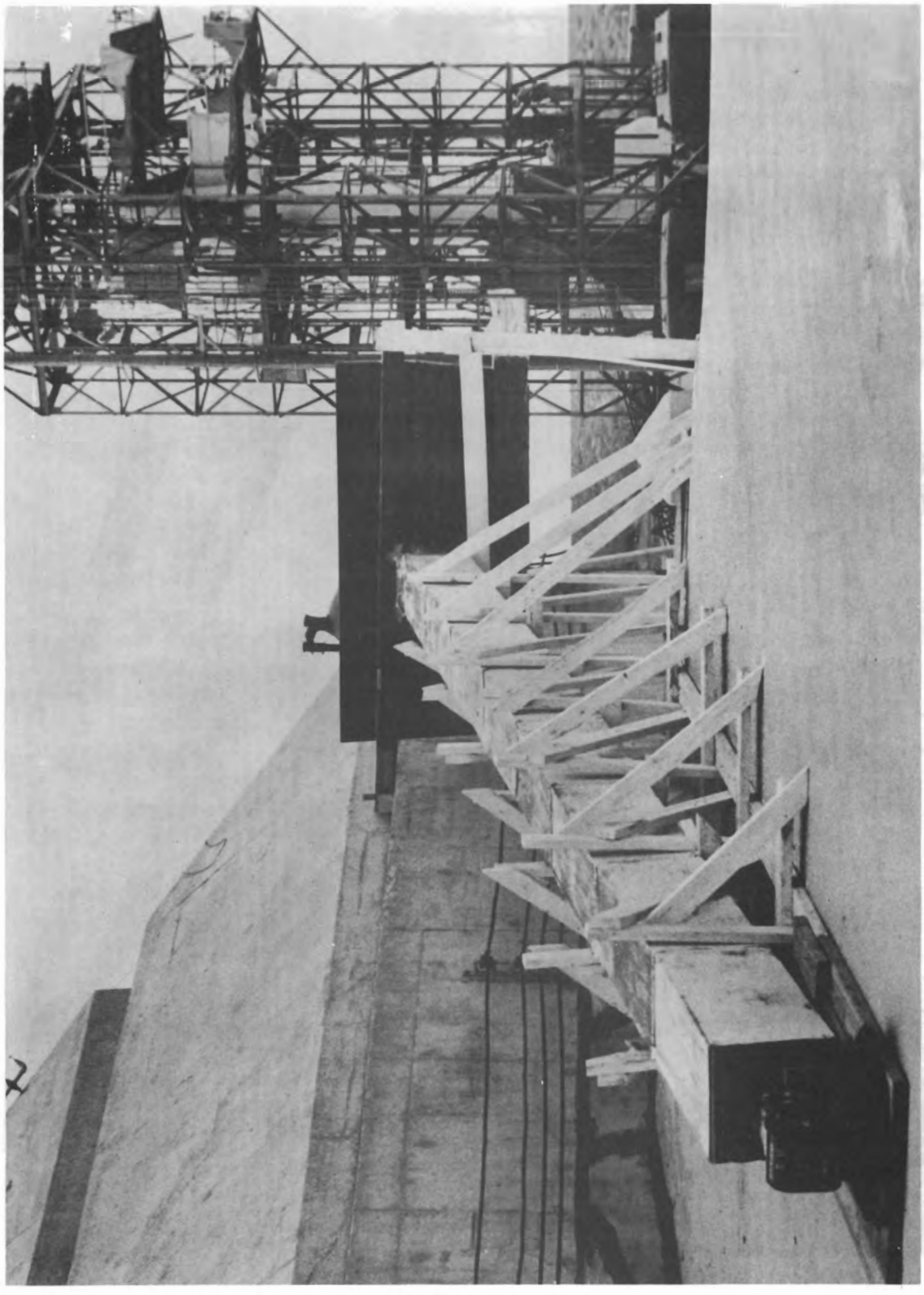

Plate 9. Blockhouse Spectrograph, General View

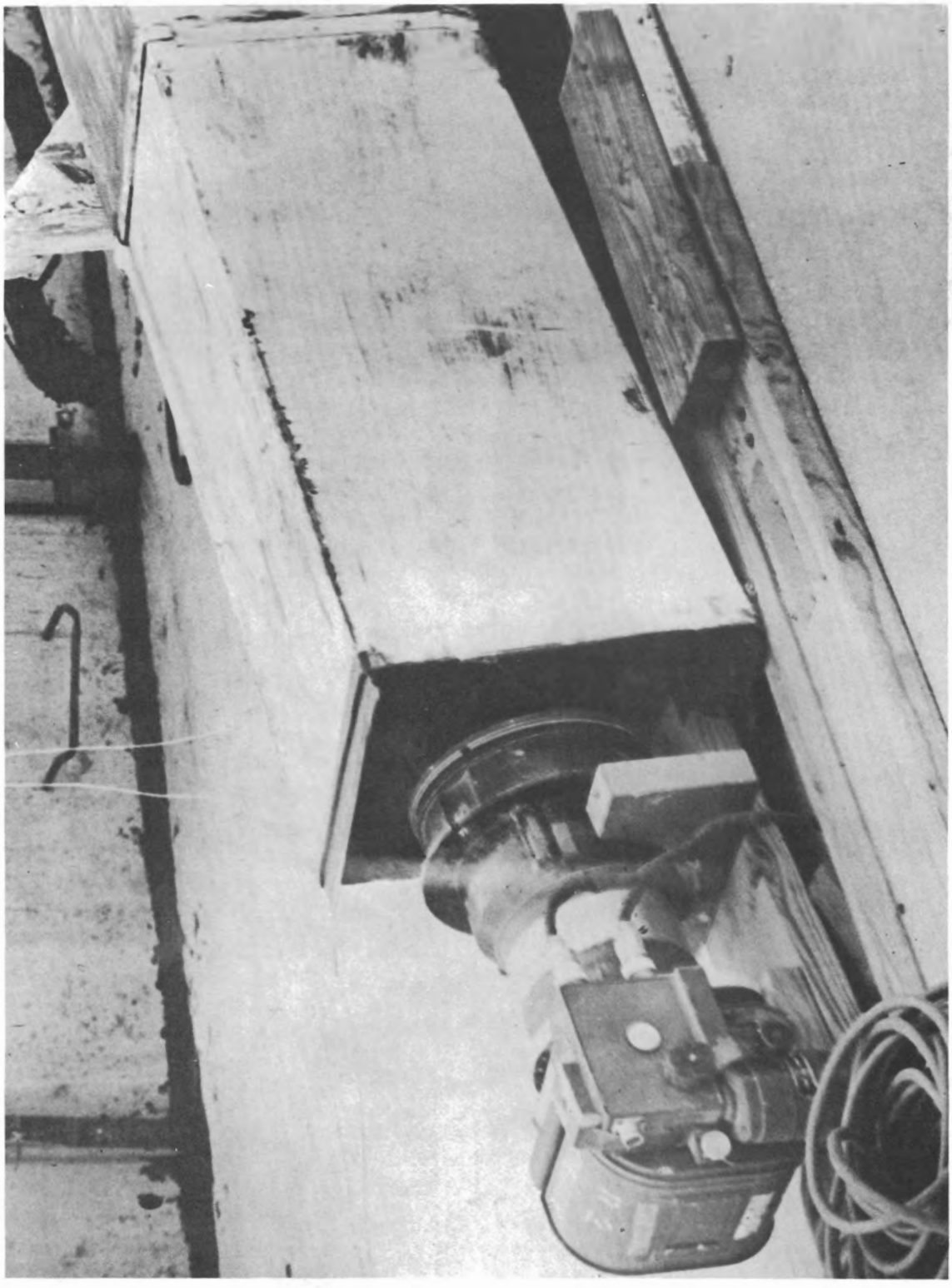

Plate 10. Blockhouse Spectrograph Camera

Plate 11. Blockhouse Spectrograph and V2 Missile

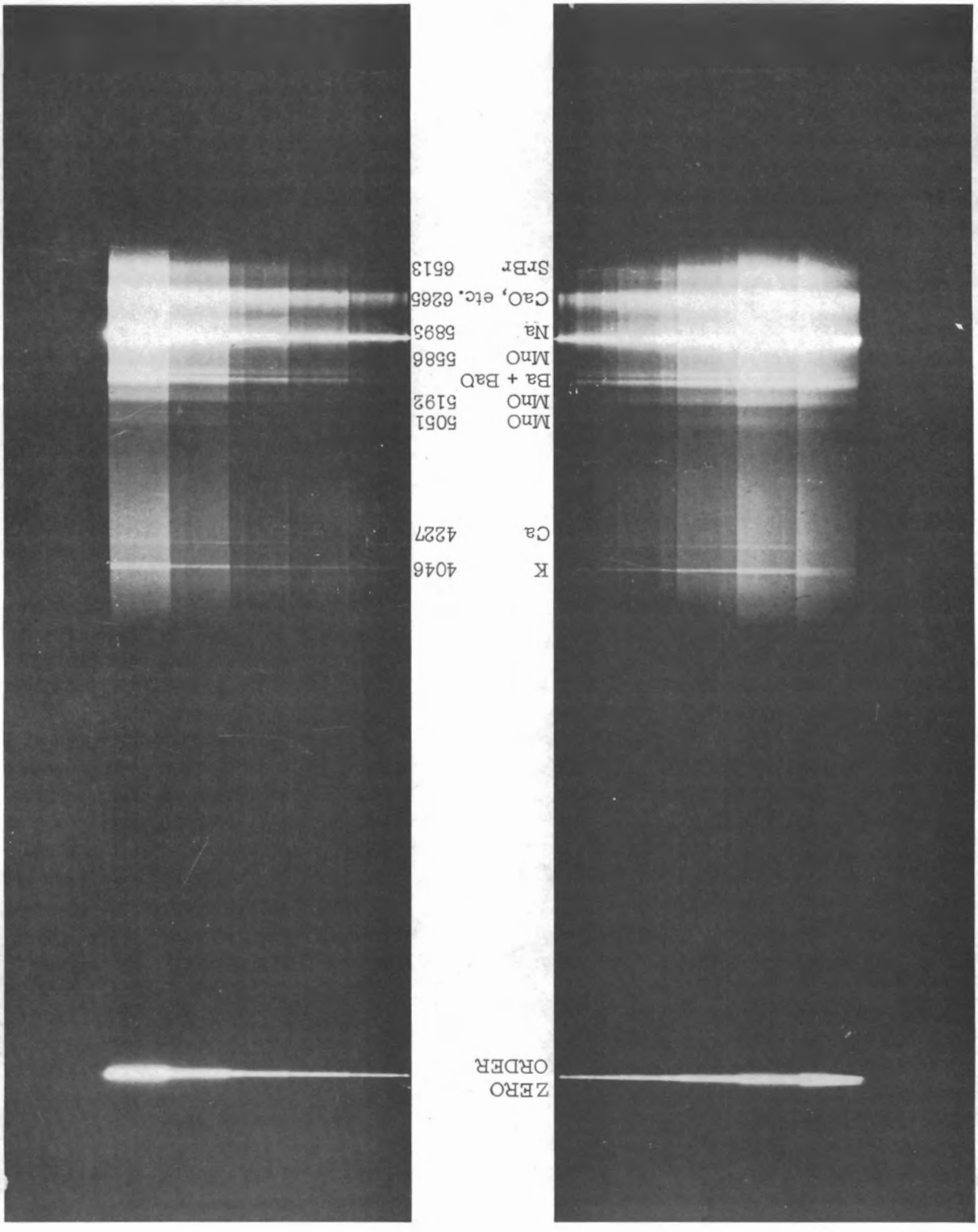

Plate 12. V2 Round 43 Predawn Firing 5 August 1948

Plate 13. V2 Firing of 26 May 1948. 103N Plate

graph by the Interior Ballistics Laboratory of the Ballistics Research Laboratories, are shown in Plate 15, together with the band indentifications. The sequence of MnO bands which appear in the A4 flame spectra apparently do not come from the fuel water.

On one occasion a small Bausch & Lomb quartz spectrograph with a quartz lens focused on the slit and a telescope for tracking was set up on a suitable tripod about 300 ft. from the rocket launching site. The rocket was tracked for the first six seconds of flight. The resulting flame spectrum, superposed on sky background, is shown in Plate 14. The jet flame has no strong emissions between Potassium 4046 and the ultraviolet quartz cutoff.

D. Identification of the Observed Jet Emissions

All of the emissions identified in the jet spectrograms are due to impurities. These are Na, K, Li, MnO, CaO, and possibly other calcium compounds. The band systems of various molecules formed by burning of the alcohol and oxygen do not appear on the spectrograms. Specifically, the bands of CH, C_2, CO, OH, and NH are not sufficiently intense to be detected on any of the spectrograms so far obtained. However, the observed emissions, particularly Sodium D, are suitable for use in the jet temperature estimates described below.

IV. THEORY OF FLAME BRIGHTNESS AND TEMPERATURE

A. Temperature Dependence of Jet Brightness

There are two approaches to this problem. The flame may be assumed to be a "grey body", with emmisivity which varies with wave length but is substantially independent of flame temperature. In this case, the Wien formula is a satisfactory approximation to Planck's equation, since the flame temperature is 2500°K or less and the wave lengths of the emissions being measured are less than 7×10^{-5} cm. When $\lambda T < 0.3$, the difference between Planck's and Wien's formulae is less than 1%. In our case, $\lambda T \leq 0.175$ so we may write the radiation from the flame at a given wave length, per unit solid angle, as

$$J_\lambda = \frac{A c_1 \epsilon}{c_2 \lambda^4} e^{-\frac{c_2}{\lambda T}} \quad \text{calories/sec./cm}^2\text{/steradian}$$

Where, if λ is expressed in centimeters,

ϵ = emmisivity of the jet.

C_1 = 2.81×10^{-13} calorie/sec/cm^2

C_2 = 1.432×10^{8} cm. degrees

A = Area of radiating surface in cm^2

or the surface brightness would be

$$I = \frac{J_\lambda}{A} = \frac{C_1 \epsilon}{C_2 \lambda^4} e^{-\frac{C_2}{\lambda T}}$$

The second approach to the flame temperature problem is thru consideration of the distribution of states in the specific molecules responsible for the emission being measured. In this case, if E_n is the excitation energy of the state n above the ground, the number of atoms (or molecules) in the state n is proportional to the Boltzmann factor provided that the energy states are in thermal equilibrium.

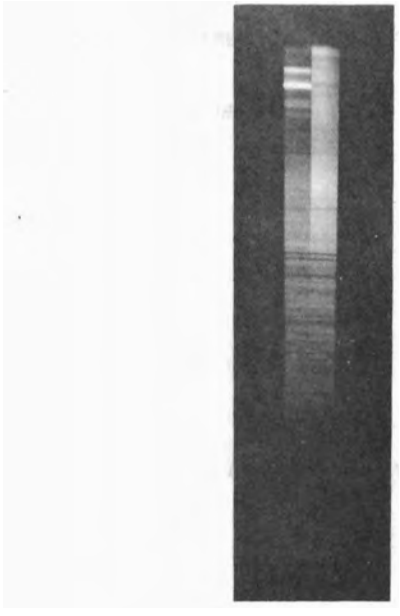

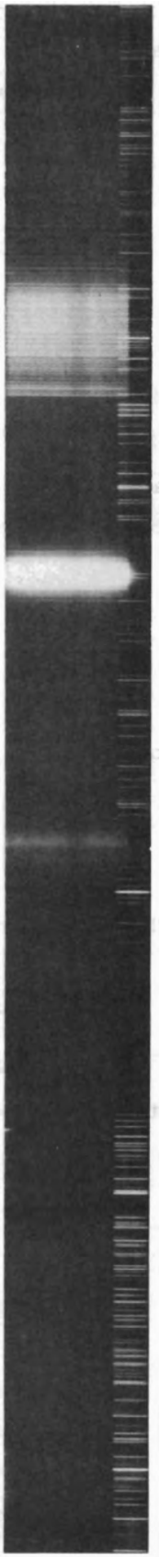

The number of atoms in the state n is also proportional to the a priori probability, or statistical weight g_n of the state n.

If N_n and N_m are the numbers of atoms in the states n and m respectively, we may write

$$\frac{N_n}{N_m} = \frac{g_n}{g_m} \quad \frac{e^{-\frac{E_n}{KT}}}{e^{-\frac{E_m}{KT}}}$$

If m is the ground state, we have the intensity I proportional to N_n and:

$$I \sim N_n = N_m \frac{g_n}{g_m} e^{-\frac{E_n}{KT}}$$

The statistical weights being equal to the degrees of degeneracy of the states to which they refer, are constants. In many cases the ratio $\frac{g_n}{g_m}$ is not large, so that when $\frac{E_n}{KT}$ is a large number, nearly all of the atoms (or molecules) are in the electronic ground state. In this case, if N is the total number of atoms involved,

$$N \approx N_m$$

and we may write approximately

$$I \sim N_n = N \frac{g_n}{g_m} e^{-\frac{E_n}{KT}}$$

Now let us compare this expression with Wien's Law. The two must differ by no more than a multiplicative constant B:

$$\frac{C_1 \epsilon}{C_2 \lambda^4} e^{-\frac{C_2}{\lambda T}} = BN \frac{g_n}{g_m} e^{-\frac{E_n}{KT}}$$

For any given λ, the two exponential terms must be identical, so we have

$$\frac{E_n}{K} = \frac{C_2}{\lambda}$$

or

$$C_2 = \frac{E_n \lambda}{K} = \frac{h \nu \lambda}{K}$$

and since

$$\nu = \frac{C}{\lambda}$$

we have

$$C_2 = \frac{hc}{K}$$

which we recognize as the definition for C_2 in Planck's expression for black body radiation, confirming the correctness of our result.

In the case of the A4 jet, the initial jet temperature at takeoff is known, and the jet temperature of the flying missile is to be determined from the observed decrease in the jet emissions as the missile rises. The ratio of the temperature T in flight to the known temperature T_o at takeoff can be determined from the expression

$$\frac{I}{I_o} = e^{\frac{-C2}{\lambda}\left(\frac{1}{T} - \frac{1}{T_o}\right)} = e^{\frac{-En}{K}\left(\frac{1}{T} - \frac{1}{T_o}\right)}$$

So that to a satisfactory degree of approximation, the consideration of molecular states and of a "grey emitter" both lead to the same expression for flame temperature in terms of takeoff temperature and observed emission intensities. This conclusion is consistent with the observed fact that the emissions of sodium atoms and of various molecules (strontium oxide, calcium oxide), as well as the continuous emission background, decrease in very nearly the same proportion as the missile rises. This is proof that the observed variation of intensity is almost independent of the structure of the emitting material, and depends almost entirely on factors which affect all radiators in the same way.

We conclude that if:

(1) Thermal equilibrium is approximated by flame conditions.

(2) $\lambda T < 0.3$

(3) $N_m \approx N$ (Nearly all atoms or molecules in the ground state).

Then the brightness of the jet will be proportional to the factor

$$e^{\frac{-E_n}{K}\left(\frac{1}{T} - \frac{1}{T_o}\right)}$$

B. Adiabatic Changes in the Jet Flame

It is clear that the jet flame, radiating energy and containing compression shock waves departs from true adiabatic conditions. The question remains whether expansions and compressions in the jet can be usefully approximated by adiabatic expressions. On inspecting the jet structure of the A4 missile at subsonic missile velocities we find a very well developed train of eight or nine Mach nodes. This train of nodes adequately testifies to the approximate reversibility of expansion and compression processes in the jet; despite the losses thru radiation and compression shocks, the expansion-and-compression cycle can repeat itself eight or more times. Thus it seems reasonable to use the adiabatic approximation to a distance of, say, fifteen feet back of the nozzle orifice. Since the jet is supersonic and the rate of rocket fuel flow is approximately constant throughout the burning time, we may assume that the state of the gas in the plane of the nozzle orifice is constant throughout the flight although this state continually refers to new parcels of gas passing thru the orifice. Now if the gas stream expands laterally while maintaining the same axial velocity, after leaving the orifice, the density of any parcel of gas will decrease proportionally to the jet diameter. And if the adiabatic approximation is used, it is possible knowing the effective ratio of specific heats and the absolute temperature of the gas in the plane of the orifice to calculate the flame temperature from the ratio

of the cross sections of "free" jet and nozzle orifice. Because every parcel of gas is in the same initial state, it is unnecessary to follow the separate parcels thru expansion and compression; any parcel of a given density will have the same temperature as any other parcel, regardless of time or place in the jet, to an approximation set by the accuracy of our adiabatic assumption.

Proceeding with the adiabatic assumption we have

$$\frac{T_2}{T_1} = \left(\frac{P_2}{P_1}\right)^{\frac{K-1}{K}}$$

T = flame temperature

P = flame pressure

$K = \frac{C_p}{C_v} = \frac{C_p}{C_p - R}$

C_p = specific heat at constant pressure

C_v = specific heat at constant volume

R = gas constant = 1.987 CHU per lb. mole, °Kelvin

From the estimates of the equilibrium products of the rocket fuel combustion and from Table IX.2, Page 372, Chemical Engineering Thermodynamics, Dodge, we have the following evaluation of K:

Substance	% of Rocket Flame	$C_{p(2300°K)}$ g.cal/g.mol.
H_2O	55.9	12
CO_2	21.5	13
CO	13.2	8.5
H_2	5.8	8.5
OH	2.8	
H	0.2	
Weighted mean C_p for rocket flame		10.16

So:

$$K = 1.24$$

$$\frac{K-1}{K} = \frac{.24}{1.24} = 0.193 \qquad (3)$$

And

$$\frac{T_2}{T_1} = \left(\frac{P_2}{P_1}\right)^{0.193}$$

Now introducing the assumption of a perfect gas, which should be a good approximation in view of the high temperature and low pressure of the jet:

$$PV = RT$$

$$\frac{P}{\rho_f} = RT$$

We obtain

$$\frac{T_2}{T_1} = \left(\frac{\rho_2}{\rho_1}\frac{T_2}{T_1}\right)^{0.193} \tag{4}$$

so:

$$\rho_2 = \rho_1\left(\frac{T_2}{T_1}\right)^{\left(\frac{1}{0.193}-1\right)} = \frac{P_1}{T_1^{4.16}}\,T_2^{4.16} \tag{5}$$

Or, solving for T:

$$T_2 = T_1\left(\frac{\rho_2}{\rho_1}\right)^{0.240} \tag{6}$$

C. General Expression for Observed Flame Surface Brightness

Let us now turn to the more detailed examination of the jet flame structure which is made possible by microphotometry of the jet flame photographs. The details of microphotometric techniques are described in the section following this one. The following development is introduced here as part of the basic theoretical material.

Let:

- I = Observed surface brightness of the jet flame.
- K = A constant depending on the observing instrument.
- T = Jet flame temperature, °Kelvin.
- t_a = Atmospheric transmission at standard temperature and pressure.
- t_f = Flame transmission at S. T. P.
- ρ_o = Atmospheric density at S. T. P.
- ρ_x = Atmospheric density at point x on the line of sight.
- ρ_f = Flame Density.
- k = Boltzmann Constant.
- ϵ = Flame emmisivity.
- E = Energy of one quantum at observed wave length.

The general expression for the observed surface brightness of the image of the jet flame in any given wave length is:

$$I = K\, t_a^{\int_0^{x_1} \frac{\rho_x}{\rho_o}\, dx} \int_{x_1}^{x_2} \epsilon\, \rho_f\, e^{-\frac{E}{KT}} t_f^{\int_{x_1}^{s} \frac{\rho_f}{\rho_o}\, dx}\, ds$$

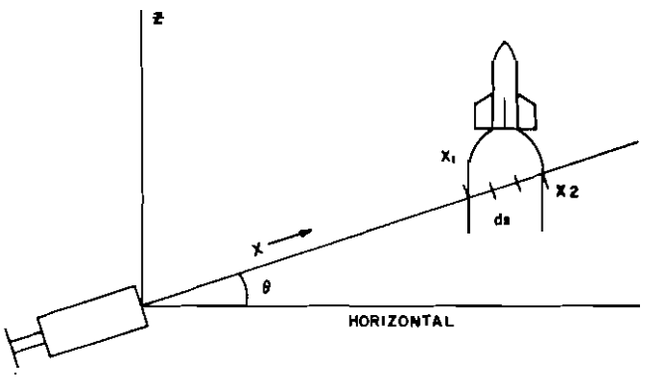

If density and temperature in the flame are assumed connected by an adiabatic law either ρ_f or T can be eliminated in terms of the other.

D. Approximate Method for Exploration of the Jet Flame Structure

In this equation for I let us concentrate our attention on the part under the integral. This part pertains to phenomena within the flame. If the flame is broken up into a finite number of volume elements, throughout each of which the temperature and density are assumed constant the integrals in (1) become series of finite numbers of terms, involving the volume elements in the path of the beam. If we use the coordinates (Z, r, ϕ) to define any particular volume element within the jet we may write:

$$I = K\, t_a^{\int_0^{x_1} \frac{\rho_x}{\rho_o}\, dx} \epsilon \sum_{\text{path}} \rho(Z, r, \phi)\, e^{-\frac{E}{KT}} t_f^{\frac{1}{\rho_{f_o}} \sum_{\text{path}} \rho_f\, \Delta x}\, \Delta s$$

The number, size, shape, and distribution of these elements will in practice depend upon the aspect of the missile, the resolution of the images used, and the purpose of the investigation being made.

Consider two photometric traces across the jet at the same distance back of the nozzle, taken from two perpendicular directions; for instance, the "broad" and "narrow" views of the flame. At each place on each curve the observed intensity I will be given by the total effect of the flame elements seen projected upon that place, as described in the above equation. Each curve involves each flame element once; both curves together involve the same element twice.

In Figure 1a are two sets of observed intensities I, representing two perpendicular lines. The oval represents the observed outline of the jet flame. With due allowance for absorption, the tabulated intensities I should be the sums of the intensities of all the flame elements projected upon it. Each element is a component of two such sums, whose values are specified in the photometric data. The array of brightness numbers in the small flame elements in Figure 1a have been adjusted by trail so that their sums approximately match the two sets of photometric data. It was assumed that absorption was negligible in the "broad" flame aspect,

and the discrepancy between the sums and the photometric data for the "narrow" aspect show the effects of increased absorption when one "leg" of the flame is seen thru the other.

Figure 1b is the same scheme using another set of data and checked with a third set of photometric I-values taken diagonally as shown.

The data for Figures 1a and 1b were all obtained from one continuous film record of a rocket that lost roll control and rotated rapidly, so that there was no problem of calibration between film records from different instruments. The two perpendicular views were obtained so close together in time that changes in intrinsic properties of the jet were relatively small. The fact that the telescope was looking obliquely upward through the jet instead of normal to the jet axis would have some moderately small effects on the results because of increased effective jet thickness and jet structure changes in an axial direction. No correction has been made for these. However Figures 1a and 1b are believed to give a qualitatively correct picture of the cross sectional distribution of the jet brightness near the brightest part of the jet.

E. Atmospheric Transmission

In the general expression for the observed jet surface brightness, the atmospheric transmission factor on the line of sight from rocket to observer is:

$$\int_0^x \frac{\rho_x}{\rho_o}\,dx \qquad \int_0^x \frac{P_x\,T_o}{P_o\,T_x}\,dx \doteq \frac{A+B}{\sin\theta}$$

$$t_a \qquad\qquad = t_a$$

where A and B refer to the parts of the optical path in the troposphere and stratosphere respectively.

We need to put the integral into more convenient coordinates insert the functional form of x, and integrate. Expressing the integral in terms of Z and θ, we get

$$\frac{1}{\rho_o}\int_0^Z \rho_Z\,\frac{dZ}{\sin\theta}$$

If one adopts the U. S. Standard Atmosphere, [8] with a constant lapse rate to the tropopause and constant temperature above one obtains for the troposphere

$$A = \int_o^{h_1} \left(1 - \frac{\rho\beta}{T_o}\right)^{\frac{g}{RB}-1} dZ$$

β = lapse rate
T_o = ground temperature
g = grav. accel.
R = gas const.
Z = altitude
h_1 = altitude of tropopause
h_2 = altitude of missile

and for the stratosphere

$$B = \frac{P}{Po}\int_{h_2}^{h_1} e^{-\frac{gZ}{RT}}\,dZ$$

Where $h_2 < h_1$, the stratosphere term is discarded and h_2 replaces h_1 as the upper limit of the troposphere term. This development neglects curvature of the Earth.

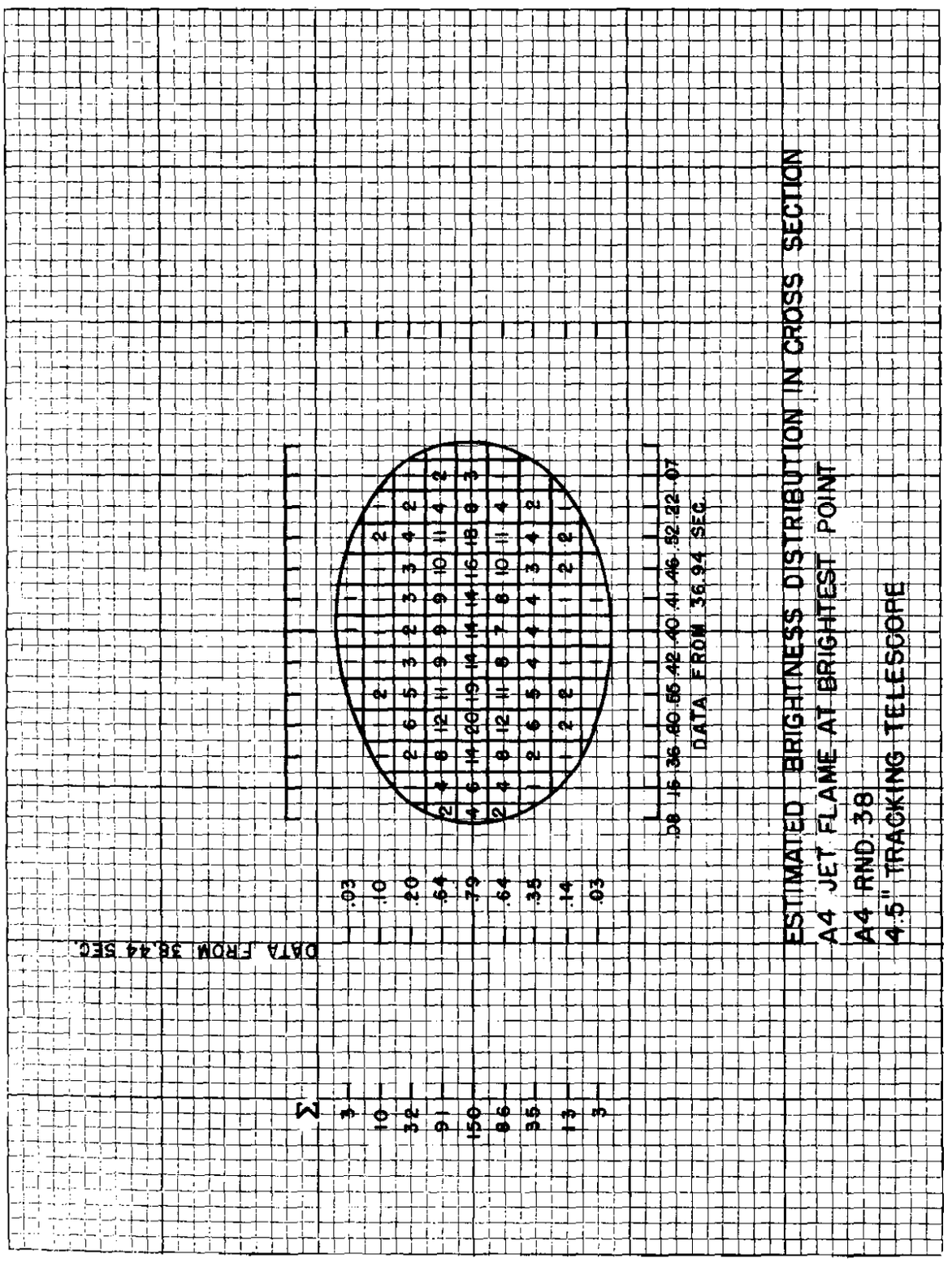
ESTIMATED BRIGHTNESS DISTRIBUTION IN CROSS SECTION
A4 JET FLAME AT BRIGHTEST POINT
A4 RND 38
4.5" TRACKING TELESCOPE
DATA FROM 36.94 SEC
DATA FROM 38.44 SEC
Σ

Fig. 1a

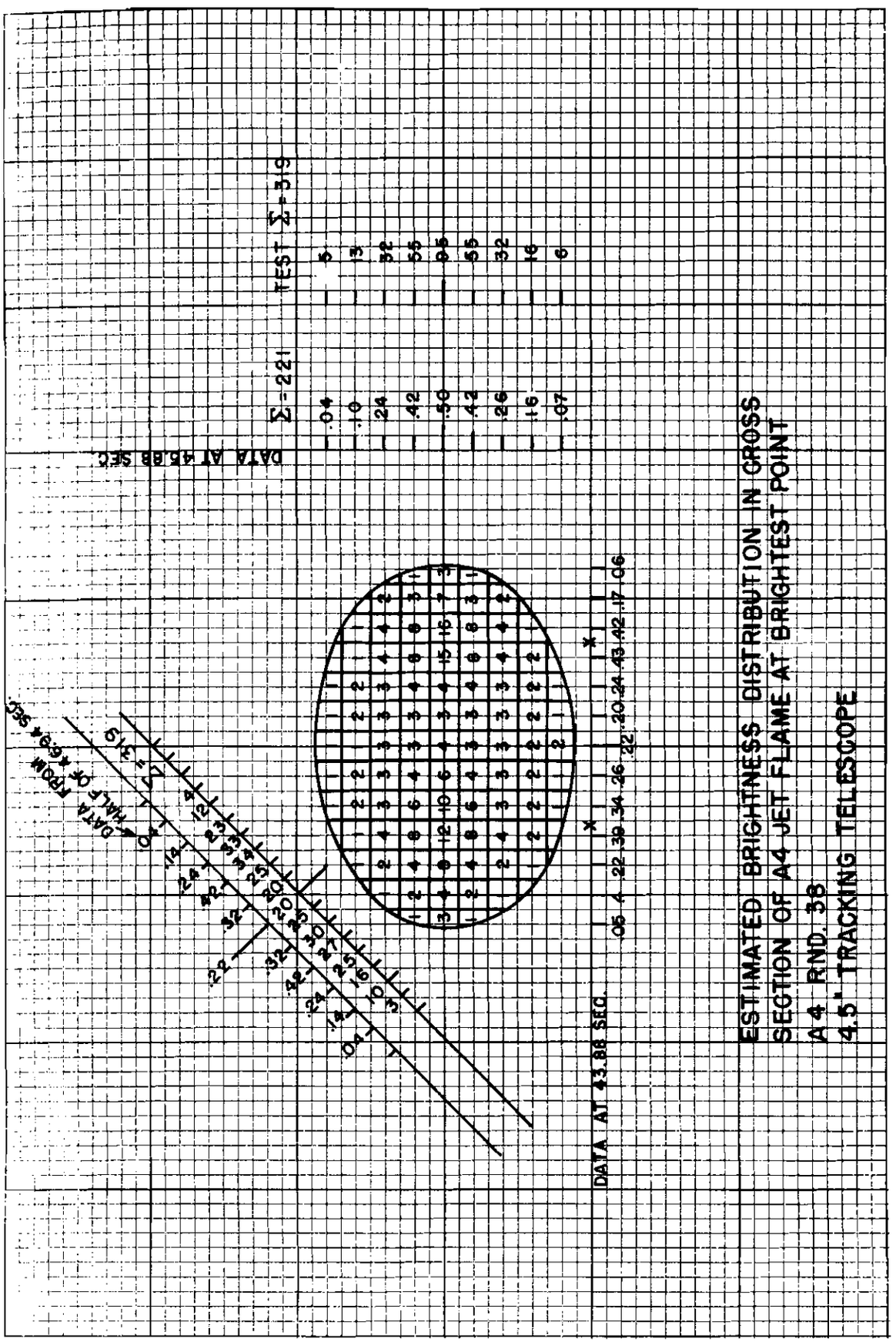
ESTIMATED BRIGHTNESS DISTRIBUTION IN CROSS SECTION OF A4 JET FLAME AT BRIGHTEST POINT
A4 RND. 38
4.5" TRACKING TELESCOPE
DATA AT 43.88 SEC.
DATA AT 45.88 SEC.
TEST Σ=319
Σ=221

Fig. Ib.

The atmospheric transmission term then becomes

$$t_a^{\frac{A+B}{\sin\theta}}$$

Integration gives at once:

$$B = \frac{PRT_1}{P_o g}\left(1 - e^{-\frac{g z}{RT}}\right)\Bigg]_{h_1}^{h_2}$$

And

$$A = \frac{T_o R}{g}\left[1-(1-\frac{Z}{T_o})^{\frac{g}{R\beta}}\right]_o^{h_1}$$

For Ta = 0.8, the stransmission in the path for various altitudes and elevation angles is given in Fig. 2.

V. MICROPHOTOMETRY OF THE SPECTROGRAMS AND DIRECT PHOTOGRAPHS

A. Microphotometric Traces

Microphotometric traces from the film records were made with a Leeds and Northrup recording microphotometer. The resolution limit of this instrument proved to be considerably smaller than the width of the narrowest detail encountered in the film records, so that all such detail could be traced out with satisfactory accuracy. The main limitation of the instrument was inability to measure sufficiently high densities with short microphotometer slits.

In the case of spectra obtained with tracking telescopes, the jet flame image was three to ten times as long as the microphotometer slit used to measure it. Except as otherwise noted, the microphotometer traces were made across the brightest part of the jet image, normal to the flame axis.

Selection of specific images for photometry was commonly done by inspection of all images within a few tenths of a second of the desired time, or of all images displaying the characteristics under study. Those images showing the best definition were then chosen for measurement.

Densities due to the jet flame were measured from a straight line interpolated between the sky background levels on each side of the image or spectrum concerned, up to the photometric trace of the spectrum or image emission in the jet flame. The density difference so measured represents light added by radiation from the jet minus light lost by absorption of the sky background behind the jet. This absorption effect is evidently small. In the first place, the missile is, thru the significant part of the burning time, so high and far away as to put most of the sky light between it and the observer, and a relatively modest part of the sky background passes thru the jet. Furthermore, if absorption in the jet were heavy, the direct photographs would show a dark streak behind the bright, emitting part of the flame. The exhaust gases, after ceasing to emit, would continue to absorb radiation from the sky background. No such dark streak has ever been observed. This result is consistent with the fact that, in photographs taken by cameras in the missile fins, the Earth can be seen thru portions of the jet flame. It is therefore concluded that absorption of sky background light in passage thru the flame is negligible.

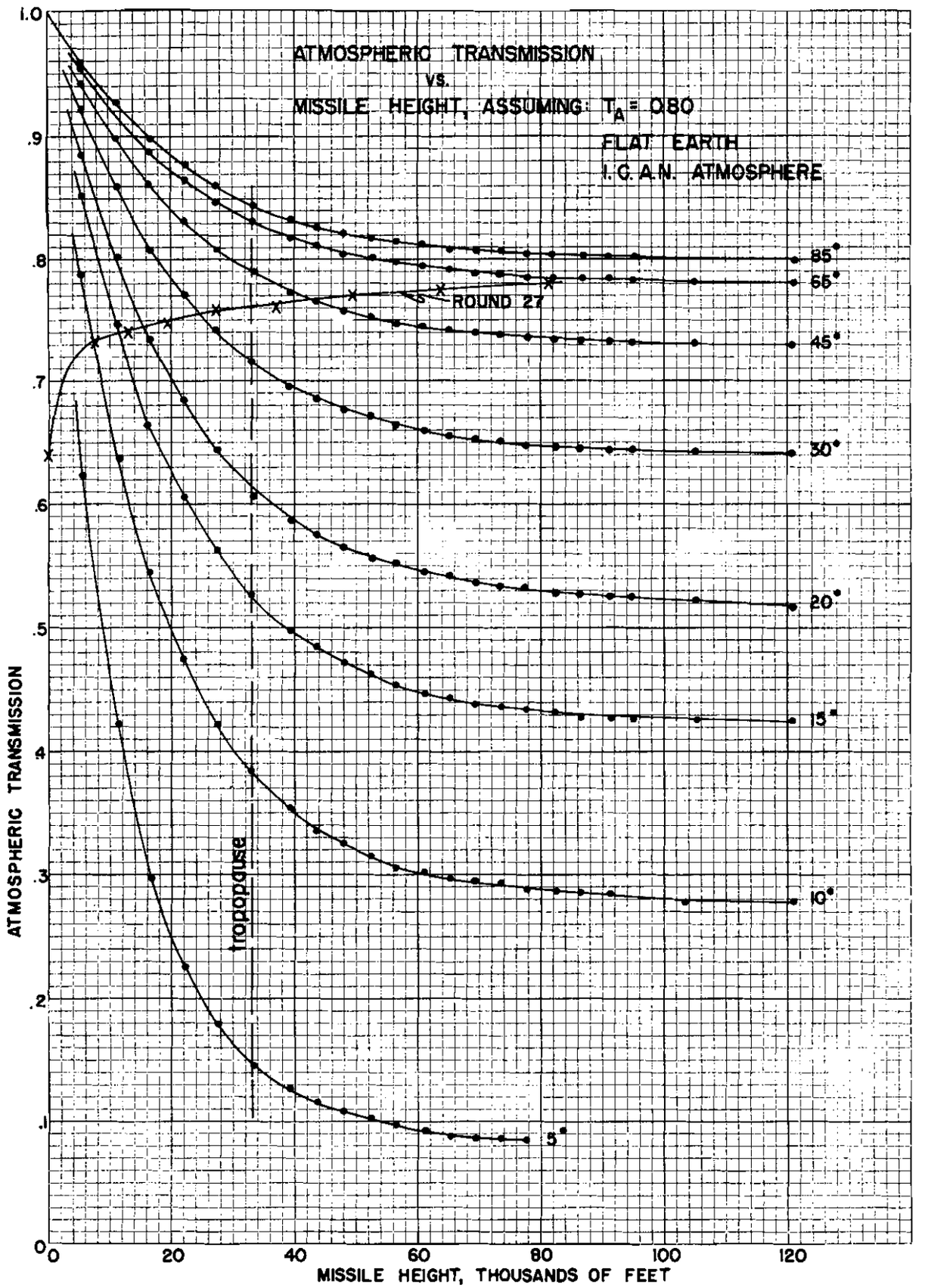
ATMOSPHERIC TRANSMISSION
VS.
MISSILE HEIGHT, ASSUMING: T_A = 0.80
FLAT EARTH
I.C.A.N. ATMOSPHERE
ROUND 27
85°
65°
45°
30°
20°
15°
10°
5°
tropopause
ATMOSPHERIC TRANSMISSION
MISSILE HEIGHT, THOUSANDS OF FEET
1.0
.9
.8
.7
.6
.5
.4
.3
.2
.1
0
0
20
40
60
80
100
120

Fig. 2

B. Exposure vs. Density

The motion picture film records of daytime firing show the jet flame spectra or direct photographs superposed on a sky background of moderate density. For several rounds, short lengths were cut from unexposed parts at the ends of the spectrographic film before development. These were impressed with sector wheel spectrophotometric exposures in the laboratory and developed along with the missile record, It was found that, for the range of densities (0 to 1.4) usually covered by the missile jet images, the density was very nearly proportional to the exposure. For all of the motion picture work, Eastman Shellburst Pan emulsion was used. This emulsion is similar to Eastman Spectroscopic 3F emulsion. Earlier photometric experience with 3F emulsion had led to a similar density-exposure linearity in the same density range. Figure 3 shows some calibration curves from films used in various rounds.

For the investigations herein discussed, the simplifying assumption of density proportional to exposure appears sufficiently accurate. This assumption was therefore adopted.

A constant exposure time (constant camera speed) for all frames in any given film was also assumed. This assumption was verified within a few percent with the aid of time marks at 1/2 second intervals on all films except those from the Mitchell theodolite and in that instrument by watching a film speed indicator dial on the instrument.

C. Sensitivity vs. Wave Length for the Telescope #1

Spectrograph

During part of its ascent the rocket leaves behind it a vapor trail. This trail, presumable composed of condensed water, appears to be white, a non-selective reflector of sunlight. Assuming the non-selectivity of this reflection, and knowing the spectral intensity distribution of sunlight as transmitted thru the atmosphere, [9] one can calculate the effective spectrograph sensitivity $\frac{\Delta \text{ density}}{\Delta \text{ intensity}}$ as a function of wave length, on the basis of the photometric curve along the vapor trail spectrum. This has been done and the result is displayed in Figure 5. The minimum around 5000 A corresponds to a sensitivity minimum in the shellburst emulsion.

Use of this curve permits the transformation of the spectrophotometric curves of the jet flame into curves showing true relative intensity at various wave lengths.

VI. CALCULATION OF JET FLAME TEMPERATURE

A. Spectrophotometric Temperature Determination

Factors included in the calculation of flame temperatures from photometric measurement of the spectograms are as follows:

(a) Atmospheric absorption between missile and observing instrument.

(b) Absorption within the flame, particularly "self-reversal".

(c) Angle ϕ between line of sight and jet axis which is related to the thickness of the jet in the line of sight.

(d) Expansion of the jet which changes the number of emitters per unit volume and the self-absorption.

(e) Rate of flow of fuel thru the rocket motor, which may also affect the density.

(f) Expansions and compressions within the jet which affect both the temperature and the density of the jet material.

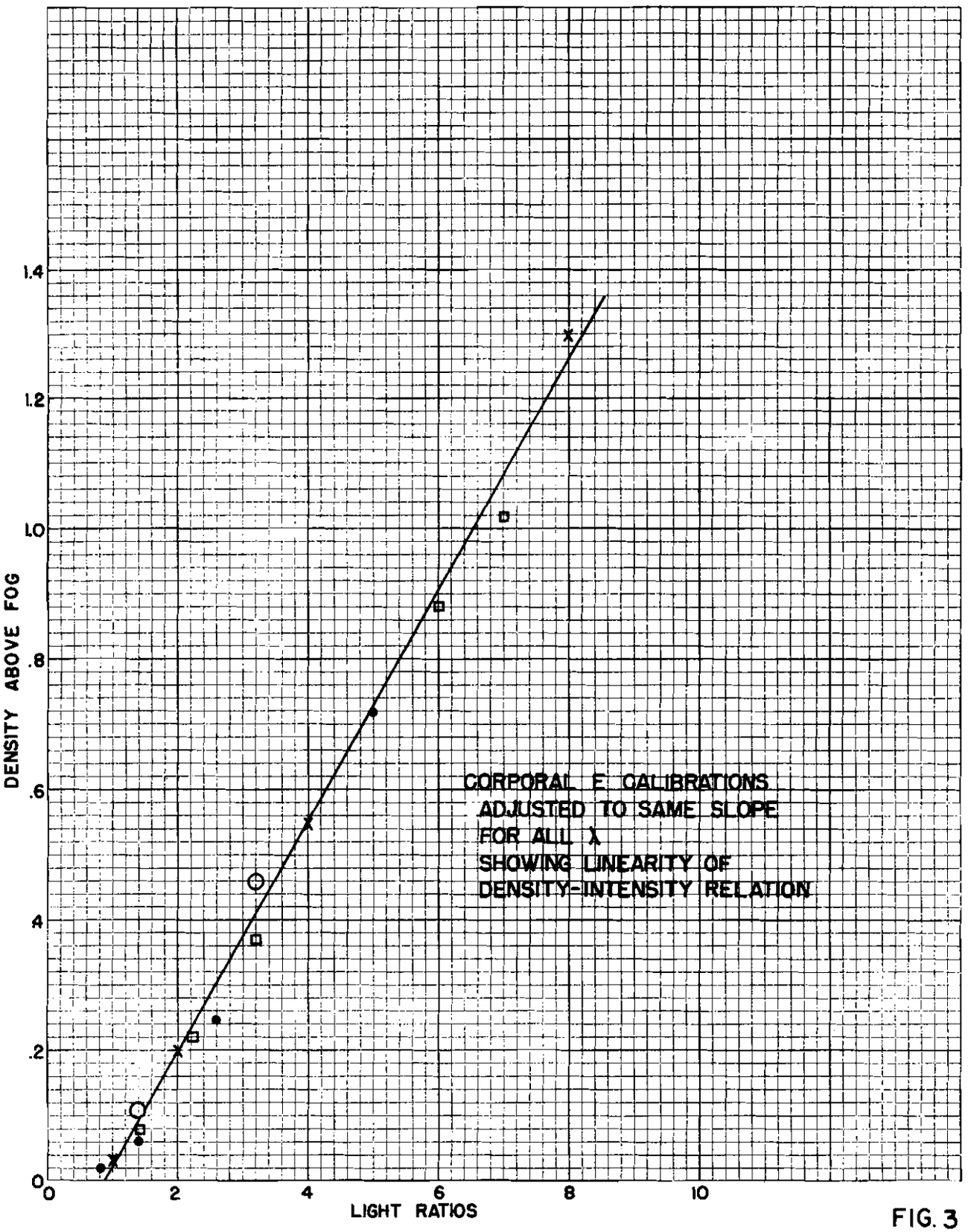
DENSITY ABOVE FOG
1.4
1.2
1.0
.8
.6
.4
.2
0
0
2
4
6
8
10
LIGHT RATIOS
CORPORAL E CALIBRATIONS
ADJUSTED TO SAME SLOPE
FOR ALL λ
SHOWING LINEARITY OF
DENSITY-INTENSITY RELATION

FIG. 3

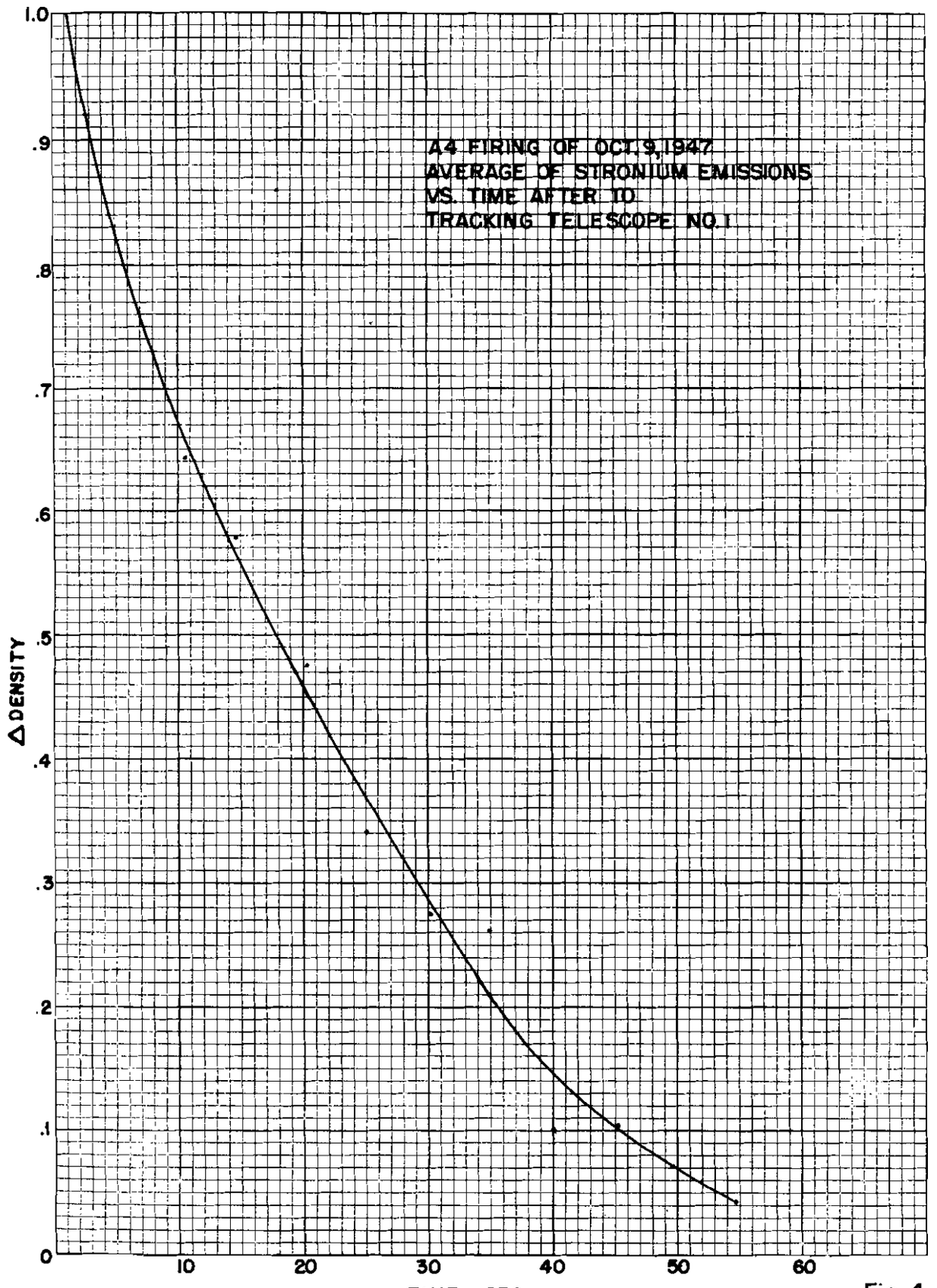
A4 FIRING OF OCT. 9, 1947
AVERAGE OF STRONTIUM EMISSIONS
VS. TIME AFTER TO
TRACKING TELESCOPE NO. 1
Δ DENSITY
1.0
.9
.8
.7
.6
.5
.4
.3
.2
.1
0
10
20
30
40
50
60
TIME – SEC

Fig. 4

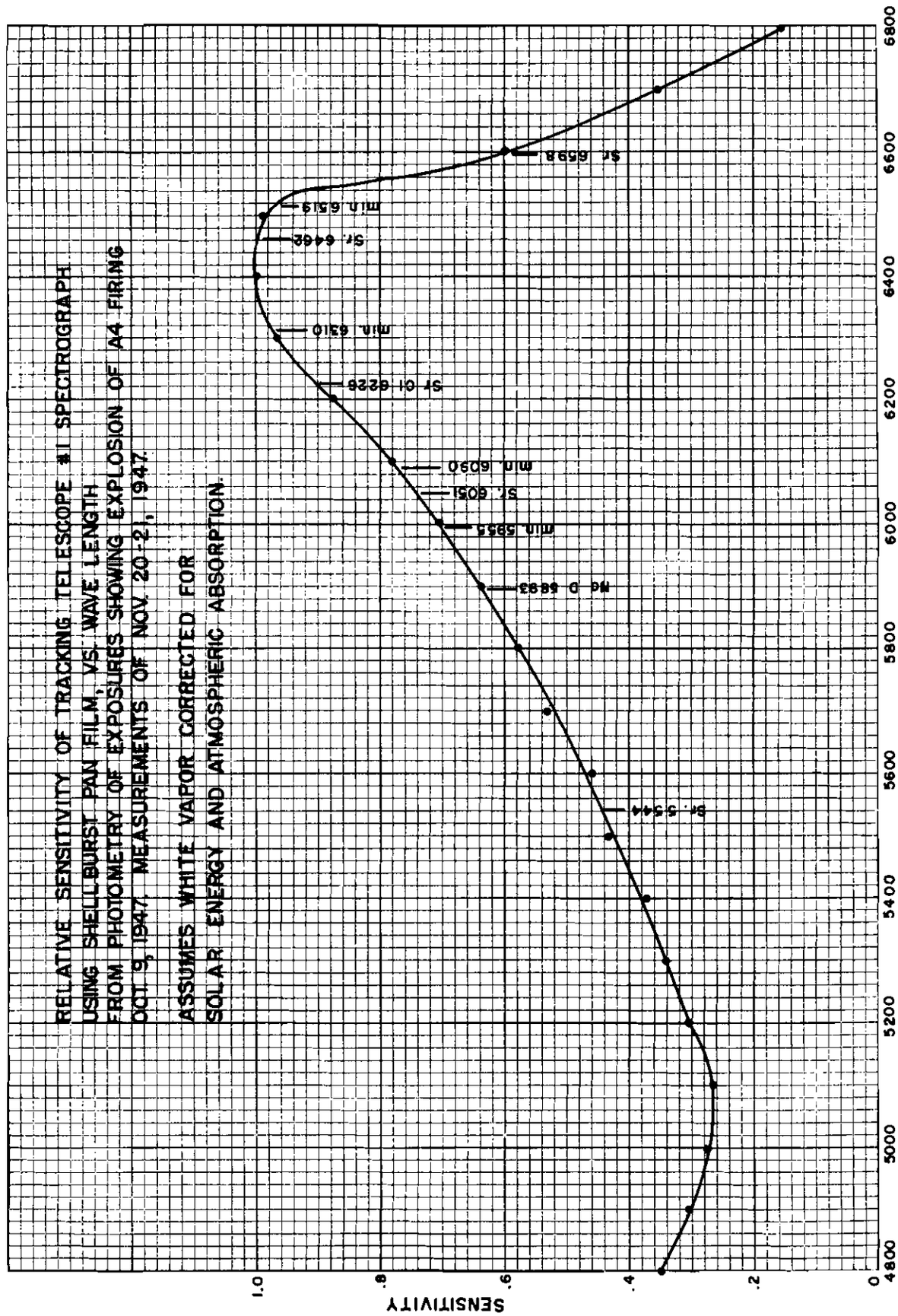
RELATIVE SENSITIVITY OF TRACKING TELESCOPE #1 SPECTROGRAPH
USING SHELLBURST PAN FILM, VS. WAVE LENGTH
FROM PHOTOMETRY OF EXPOSURES SHOWING EXPLOSION OF A4 FIRING
OCT. 9, 1947. MEASUREMENTS OF NOV. 20-21, 1947.
ASSUMES WHITE VAPOR CORRECTED FOR
SOLAR ENERGY AND ATMOSPHERIC ABSORPTION.
Sr. 6598
min. 6519
Sr. 6466
min. 6310
Sr Oi 6228
min. 6090
Sr. 6051
min. 5853
Na D 5893
Sr. 5544
SENSITIVITY
1.0
.8
.6
.4
.2
0
WAVE LENGTH Å
6800
6600
6400
6200
6000
5800
5600
5400
5200
5000
4800

Fig. 5

In this discussion the part of the jet involved will be a zone scanned by the microphotometer normal to the jet axis across the brightest part of the jet. The temperature under discussion will be an "average" one associated with this brightest part, or the zone in which it lies. The effect of jet structure will not be dealt with in detail. A suitable expression taking into consideration the above-listed factors for a temperature of the brightest area based on jet surface brightness, is:

$$\frac{I}{I_o} = \frac{t_a^{\frac{A+B}{\sin\theta}} \; \tau_f \; D\sqrt{F} \; \sin\phi_o}{t_a^{\left(\frac{A+B}{\sin\theta}\right)_o} \; \tau_f \; D_o\sqrt{F_o} \; \sin\phi} \; e^{-\frac{En}{K}\left(\frac{1}{T} - \frac{1}{T_o}\right)}$$

where:

I = observed intensity from microphotometer record

F = rate of rocket fuel flow

T = flame temperature

t = transmission of one atmosphere

τ = $\frac{\text{brightness observed}}{\text{brightness without flame absorption}}$

θ = angle of elevation

ϕ = angle between line of sight and jet axis

D = flame diameter as seen from observing position

and the subscript o refers to initial conditions. The inclusion of the term D/D_o takes care of density changes due to changing atmospheric pressure on the jet surface, and also partially of changes of rate of flow of the rocket fuel. Changes in rocket fuel flow have very little effect on the jet velocity; their principal result is a change of the jet pressure at the nozzle exit. Thus, increased fuel flow results in increased exit pressure, which in turn leads to a greater diameter of the jet after expansion into the atmosphere, so that a given percentage increase in rocket fuel flow causes the amount of material in the optical path thru the beam to increase by only the square root of this percentage. Also, the rate of fuel flow is intended to be and in fact is constant within a few percent throughout the burning time.

It has been remarked earlier that the absorption of skylight passing through the jet seems undetectable. This is not the case with the absorption of jet radiations on their way thru the jet, where the specific emissions generated by the jet meet with atoms of the kind that produced them and in a state suitable to to reabsorb them. The nature of the jet structure provides means to determine approximately the self-transmission τ_f. As the jet flame broadens into two bilaterally symmetrical parts, the view of the broad side of the flame shows two bright "cores" standing side by side and obscured by only a thin veil of jet material. In the cases where the jet loses roll control, this view alternates rapidly with the "edge-on" aspect, in which the light from one bright core is reduced by having to traverse the material of the other bright core which is obscuring it. If I is the intensity of each bright core as seen broadside, then, if there were no absorption, the maximum intensity of the two seen edge-on, or superposed would be 2I. Observation shows the actual edge-on intensity as less than this, and an approximate value for the light absorb-

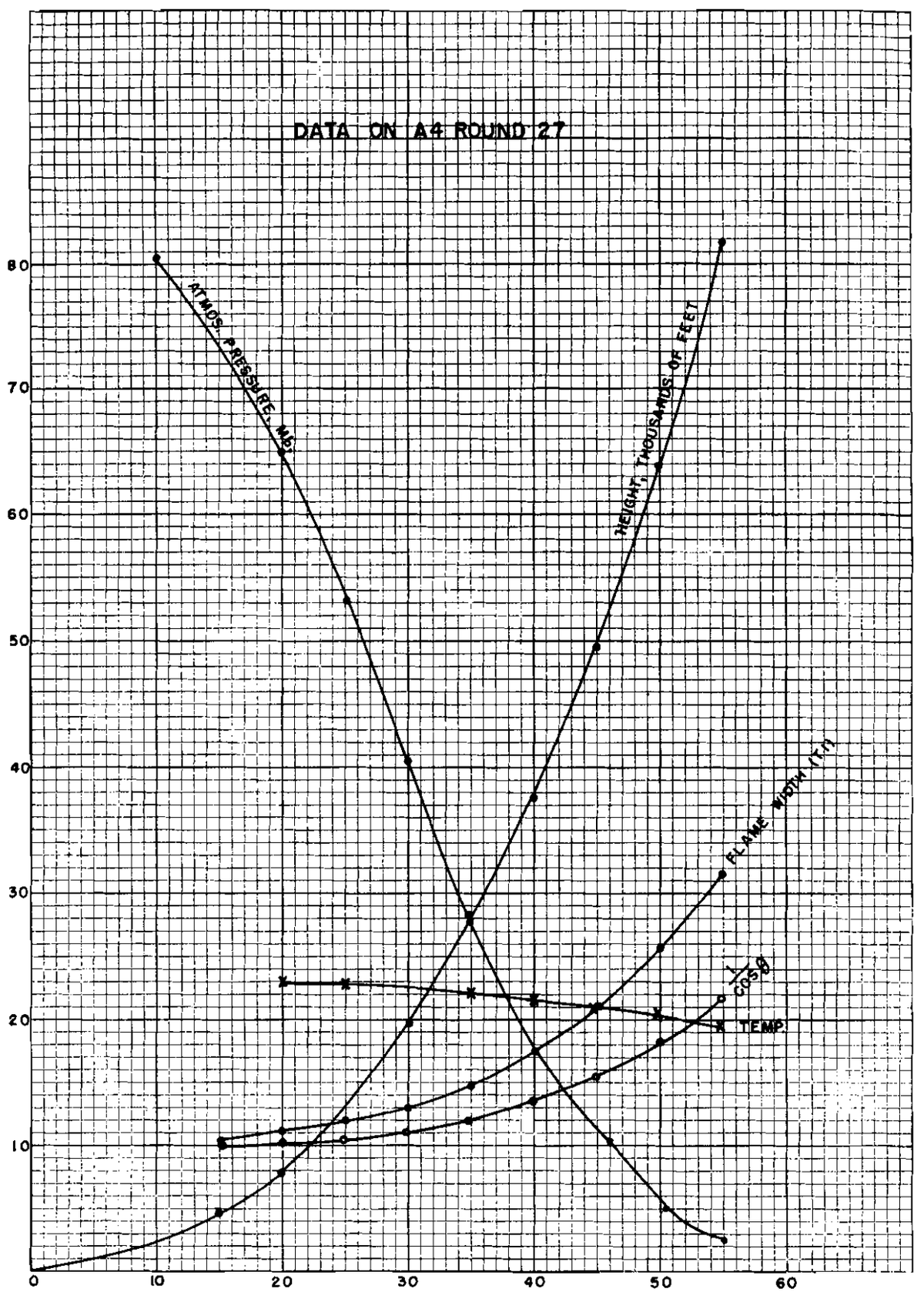
DATA ON A4 ROUND 27
ATMOS. PRESSURE - MB.
HEIGHT, THOUSANDS OF FEET
FLAME WIDTH (FT.)
1/COSθ
TEMP.
80
70
60
50
40
30
20
10
0
10
20
30
40
50
60
SECONDS AFTER To

Fig. 6

ed in passing thru the front core as

$$\Delta I = 2I - I_E$$

where I_E is the observed intensity of the jet viewed edgewise.

And the transmission of the front core is

$$\frac{I - \Delta I}{I} \lessapprox \tau_f$$

This quantity turns out to be about 0.6. The jet self-absorption is not sufficient to seriously alter the jet temperature estimates. Even if ϕ falls as low as 30°, the change in brightness due to self-absorption of the jet viewed broadside will be less than 20%, corresponding to a jet temperature error of about 20° K. Actually, when the measurements are made on the "broad" view of the flame, as was the case, it is probable that the effective τ_f is about 0.9. Therefore, flame self-absorption has a negligible effect upon the computed flame temperature.

In view of the above discussions of fuel flow and self-absorption we may write to sufficient approximation for the temperature of the brightest area of the jet:

$$\frac{I}{I_o} = t_a^{\left(\frac{A+B}{\sin\theta} - \frac{A_o + B_o}{\sin\theta_o}\right)} \frac{\sin\phi_o}{\sin\phi} \frac{D}{D_o} e^{-\frac{E_n}{KT}\left(\frac{1}{T} - \frac{1}{T_o}\right)}$$

In practice it may occur that atmospheric transmission during the first few seconds of flight is much less than than the calculated value due to a haze layer near the ground. In this case, the transmission can be obtained empirically by observation of the apparent brightness of the missile body whose true brightness usually will not change greatly during the period in question. It is possible to allow for this by writing

$$t_a^{\frac{A+B+C}{\sin\theta}} \qquad \text{instead of } t_a^{\frac{A+B}{\sin\theta}}$$

where t_a^C is the vertical transmission of the haze layer, but the more practical procedure is to neglect C at higher θ and allow for it directly from missile body observations at lower θ.

Another way to obtain a value of the jet temperature is to consider the integrated light over the path traversed by the photometer slit across the jet. This temperature should be somewhat lower than that for the "brightest area" described above. The "integrated light" method has some advantages. It is more representative of all of the flame material, and it is not much affected by image quality.

If L is the integral under the microphotometer curve, we may write

$$\frac{L}{L_o} = t_a^{\left(\frac{A+B}{\sin\theta} - \frac{A_o+B_o}{\sin\theta_o}\right)} \frac{R_o}{R} \frac{\sin\phi_o}{\sin\phi} e^{-\frac{E_n}{K}\left(\frac{1}{T} - \frac{1}{T_o}\right)}$$

Where R = slant range from missile to observer.

Note that, if the axis of the missile is vertical, and the missile flies on a vertical path, R sin ϕ is a constant, the distance from launching point to observer. Since the missile axis and path are both almost vertical,

$$\frac{R_o \sin\phi_o}{R \sin\phi} \approx 1$$

and to a fair approximation,

$$\frac{L}{L_o} = t_a^{\left(\frac{A+B}{\sin\theta} - \frac{A_o+B_o}{\sin\theta_o}\right)} e^{-\frac{E_n}{K}\left(\frac{1}{T} - \frac{1}{T_o}\right)}$$

B. Discussion of Jet Temperature and Diameter Measurements

1. General

Since the rocket motor performance remains constant throughout the burning time, it is reasonable to seek an explanation for the jet changes in terms of the changes in missile velocity and in ambient atmospheric pressure around the missile. Two jet flame parameters which change conspicuously are the jet temperature and jet diameter.

We have now to seek the relationship between:

Flame Parameters	and	Missile Parameters
(Temperature		(Atmospheric Pressure
(Cross Section		(Missile Velocity

To initiate this search we shall provisionally adopt the following assumptions:

a. Material in the jet flame behaves according to the above-developed adiabatic expressions, so far as temperature, pressure, and volume are concerned.

b. Visible radiation from the jet flame arises from thermal excitation only and is governed by the radiation equations given above.

c. At the places where jet radiation and diameter were measured, the jet pressure was uniform over the jet cross section and equal to the ambient atmospheric pressure at the altitude of the missile.

2. Jet Cross Section vs Atmospheric Pressure

By measurements of the jet diameter it is possible to determine the jet cross section. This process is complicated by the fact that the jet at supersonic velocities is not round but roughly elliptical, with a comparatively faint outer boundary along the minor axis. Careful measurements (Fig. 7) of the jet images for rounds in which the jet flame is strongly exposed (Round 27, in which the jet intensity is enhanced by strontium, and some firings near twilight with a favorable jet-to sky intensity ratio) indicate that the ratio of minor to major cross sectional axes does not fall much below 0.8 and remains fairly constant between 30 and 50 seconds.

Therefore, the jet cross section will be proportional to the square of the major jet diameter within less than 10% error. If our assumptions are correct, the square of the jet major axis should be almost pro-

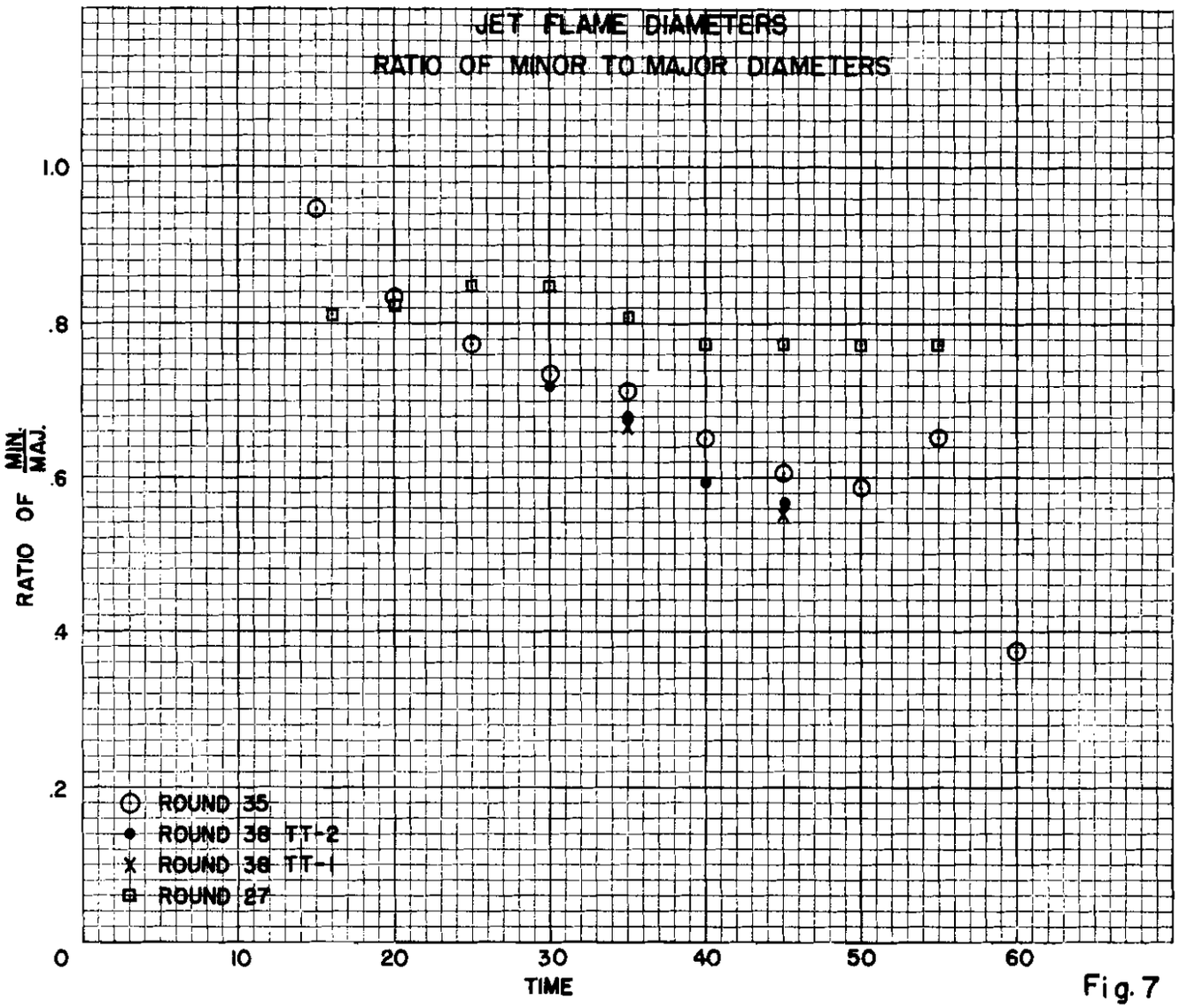

Fig. 7

portional to the reciprocal of the atmospheric pressure at the height of the missile. More nearly, it should follow the adiabatic equation

$$\frac{V_2}{V_1} = \left(\frac{P_1}{P_2}\right)^{0.81}$$

Reference to Figures 9 and 9a shows the jet cross sections measured for Rounds 24, 27, and 35 compared with $\frac{P_1}{P_2}$ and $\left(\frac{P_1}{P_2}\right)^{0.81}$, where $\frac{P_1}{P_2}$ is the ratio of atmospheric pressure on the ground and at the missile. It is seen that the jet cross section agrees very well with $\frac{P_1}{P_2}$ and fairly well with $\frac{P_1}{P_2}^{0.81}$ up to a missile altitude of about 50,000 ft. and a time of about 45 or 50 sec. after takeoff. Between altitudes of

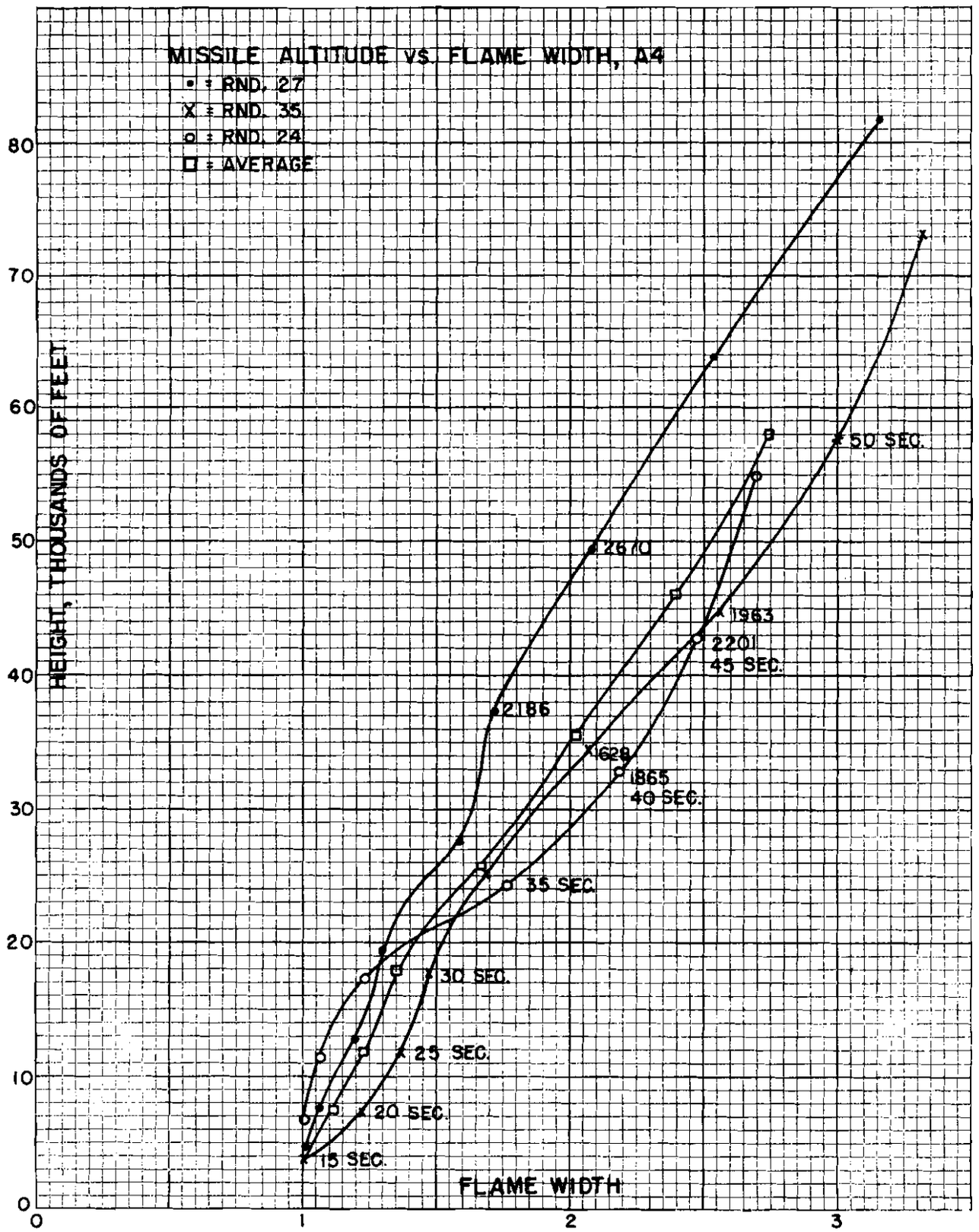
MISSILE ALTITUDE VS. FLAME WIDTH, A4
• = RND. 27
X = RND. 35
o = RND. 24
□ = AVERAGE
HEIGHT, THOUSANDS OF FEET
FLAME WIDTH
0
10
20
30
40
50
60
70
80
1
2
3
2670
2186
1963
2201
45 SEC.
1628
1865
40 SEC.
35 SEC.
30 SEC.
25 SEC.
20 SEC.
15 SEC.
50 SEC.

Fig. 8

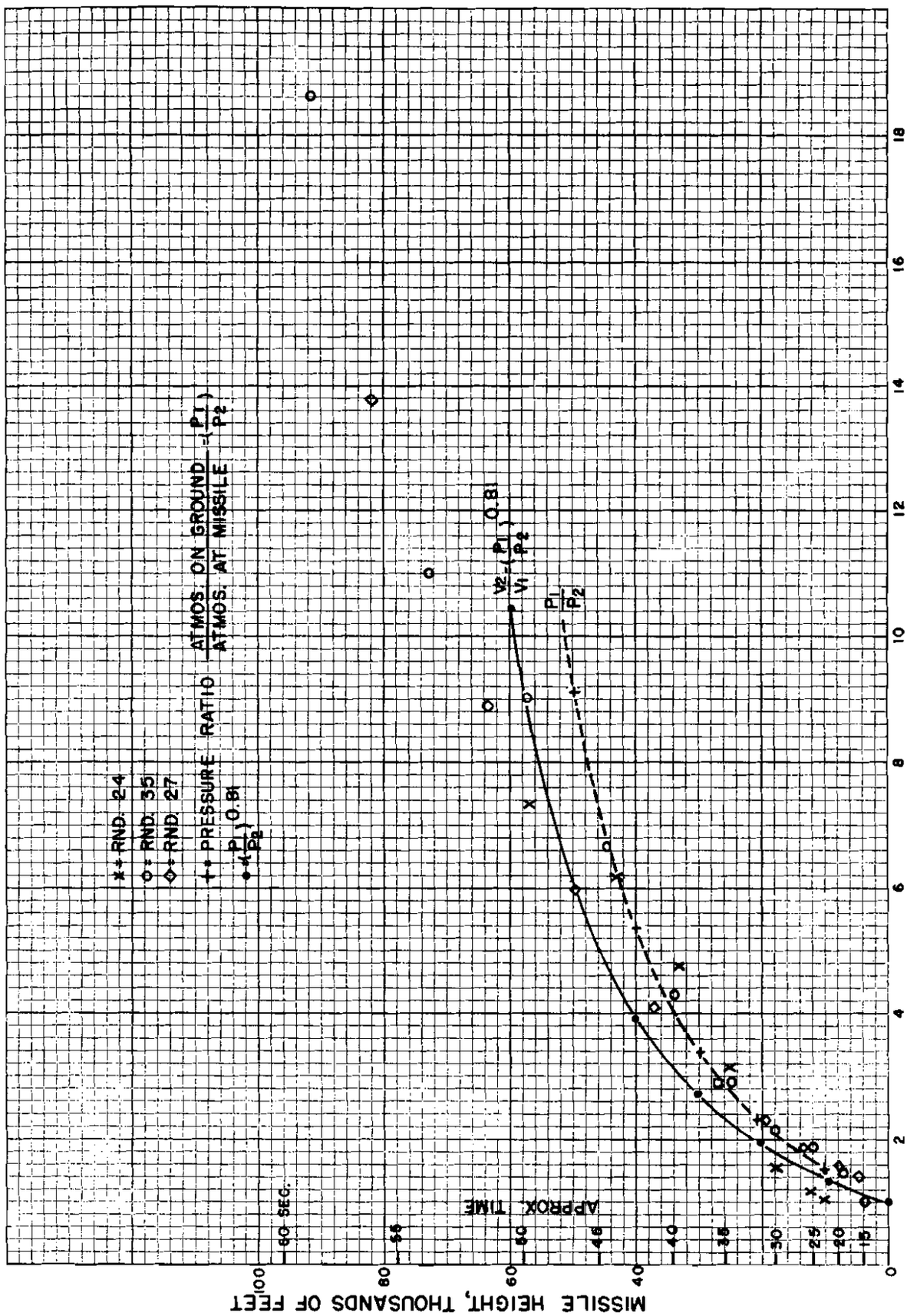
MISSILE HEIGHT, THOUSANDS OF FEET
APPROX TIME
60 SEC.
JET CROSS SECTION
x = RND. 24
◇ = RND. 35
◇ = RND. 27
+ = PRESSURE RATIO ATMOS. ON GROUND / ATMOS. AT MISSILE
● = P1/P2 0.81
V2=(P1/P2) 0.81 V1
P1/P2

Fig. 9

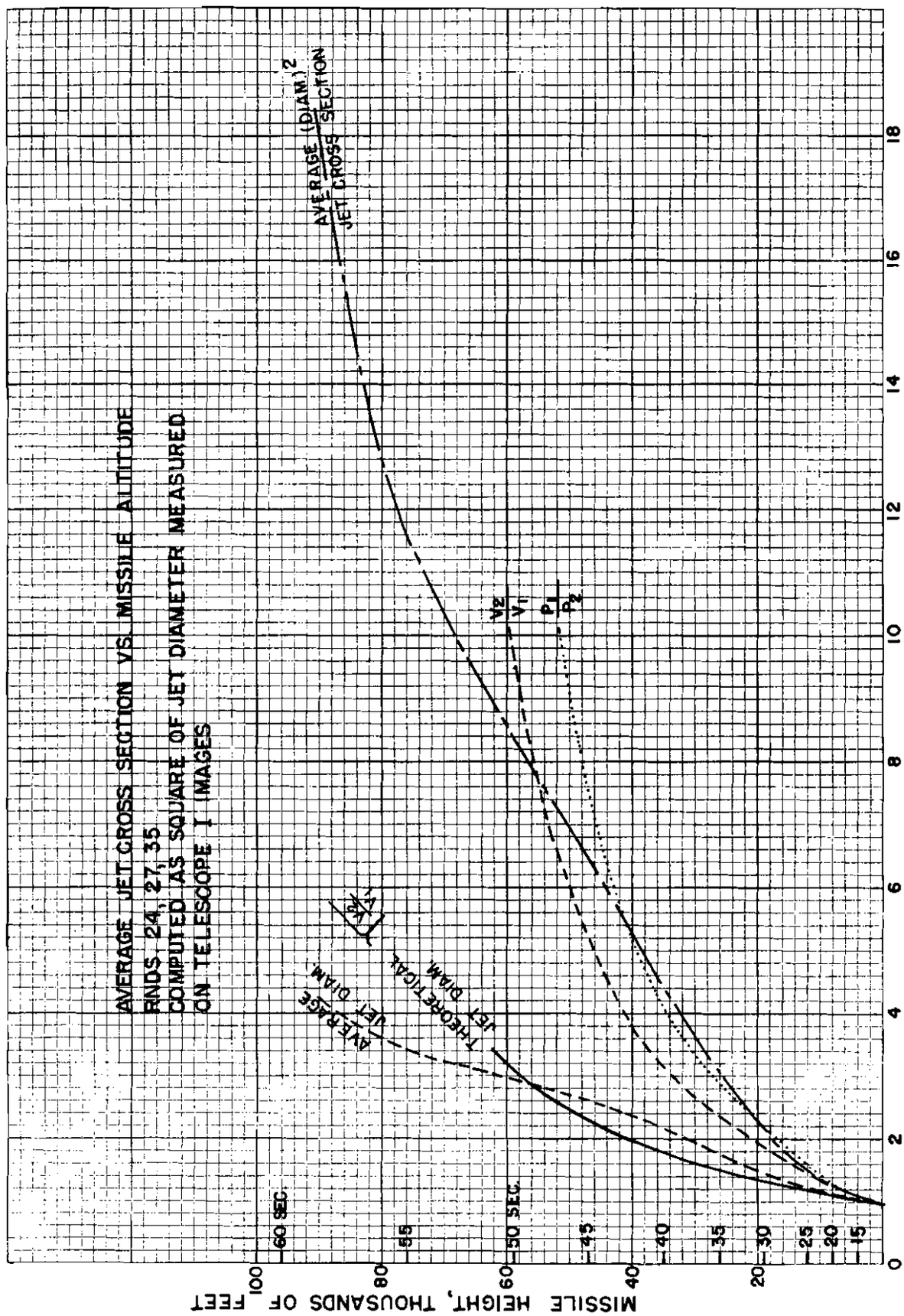
AVERAGE JET CROSS SECTION VS. MISSILE ALTITUDE
RNDS. 24, 27, 35
COMPUTED AS SQUARE OF JET DIAMETER MEASURED
ON TELESCOPE I IMAGES
AVERAGE (DIAM.)² JET CROSS SECTION
$\frac{2A}{V_1}\frac{P_1}{P_2}$
THEORETICAL JET DIAM.
AVERAGE JET DIAM.
60 SEC.
50 SEC.
MISSILE HEIGHT, THOUSANDS OF FEET
JET CROSS SECTION

Fig. 9a

50,000 and 100 000 feet (times between 50 and 60 seconds) the jet flame diameter does not increase as rapidly as theory would predict.

3. Jet Temperature: Comparison of Results from Spectrographic, Atmospheric Pressure, and Jet Cross Section Measurements

In order to use the above-developed formulae for spectrographic determination of flame temperature, it is necessary to know To, the flame temperature at takeoff. Temperature measurements made by others on static firings of rocket motors smaller than but similar to the A4 yield results between 2200°K and 2500°K. A value of To = 2500°K has been adopted for the calculations here presented.

Spectrographic flame temperature estimates have been made for Rounds 27, 28, and 34. The results, plotted against atmospheric pressure at the missile height are presented in Figure 10.

We now turn to the calculation of jet flame temperature from the adiabatic relation and the assumption of a pressure uniform over the jet cross section and equal to the ambient atmospheric pressure around the missile. The appropriate equation is

$$\frac{T_2}{T_1} = \left(\frac{P_2}{P_1}\right)^{0.19}$$

which is graphed in Figure 11.

This same relation is plotted in Figure 10 for comparison with the photometrically determined temperatures.

It is seen that the two kinds of temperature calculations yield qualitatively similar curves but that the spectrographic temperatures tend to be higher than the "pressure" temperatures, especially for Rounds 27 and 28 and at higher altitudes.

Recalling that the measured jet cross section was smaller than that calculated on the basis of jet pressure assumed equal to ambient atmospheric pressure, we see that the smaller observed jet diameter might be consistent with the higher observed spectrographic temperature. We conclude that while the assumption of jet pressure equal to ambient atmospheric pressure was a useful initial approximation, it must now be modified to account for the residual discrepancy between observation and simple theory. This we are the more willing to do because inspection of the jet flame images shows that in fact the jet was probably still expanding at the place where the diameters were measured, and it was certainly still expanding at the cross section of greatest jet brightness, where the photometric traces were taken. The corresponding outward slope of the jet surface would be associated with a greater-than-ambient pressure in the supersonic air flow around the jet. The resulting higher jet pressure would go along with the observed higher jet temperature and smaller jet cross section.

4. Jet Temperature vs Jet Diameter: An Experimental Value for the Jet C_p.

Let us now turn to the comparison of spectrographic jet temperature with the observed cross section of the jet. We shall do this with the aid of a new assumption, which is:

"The axial component of velocity of the jet gases at the cross section cut by the photometric trace is the same for all observations of a given round."

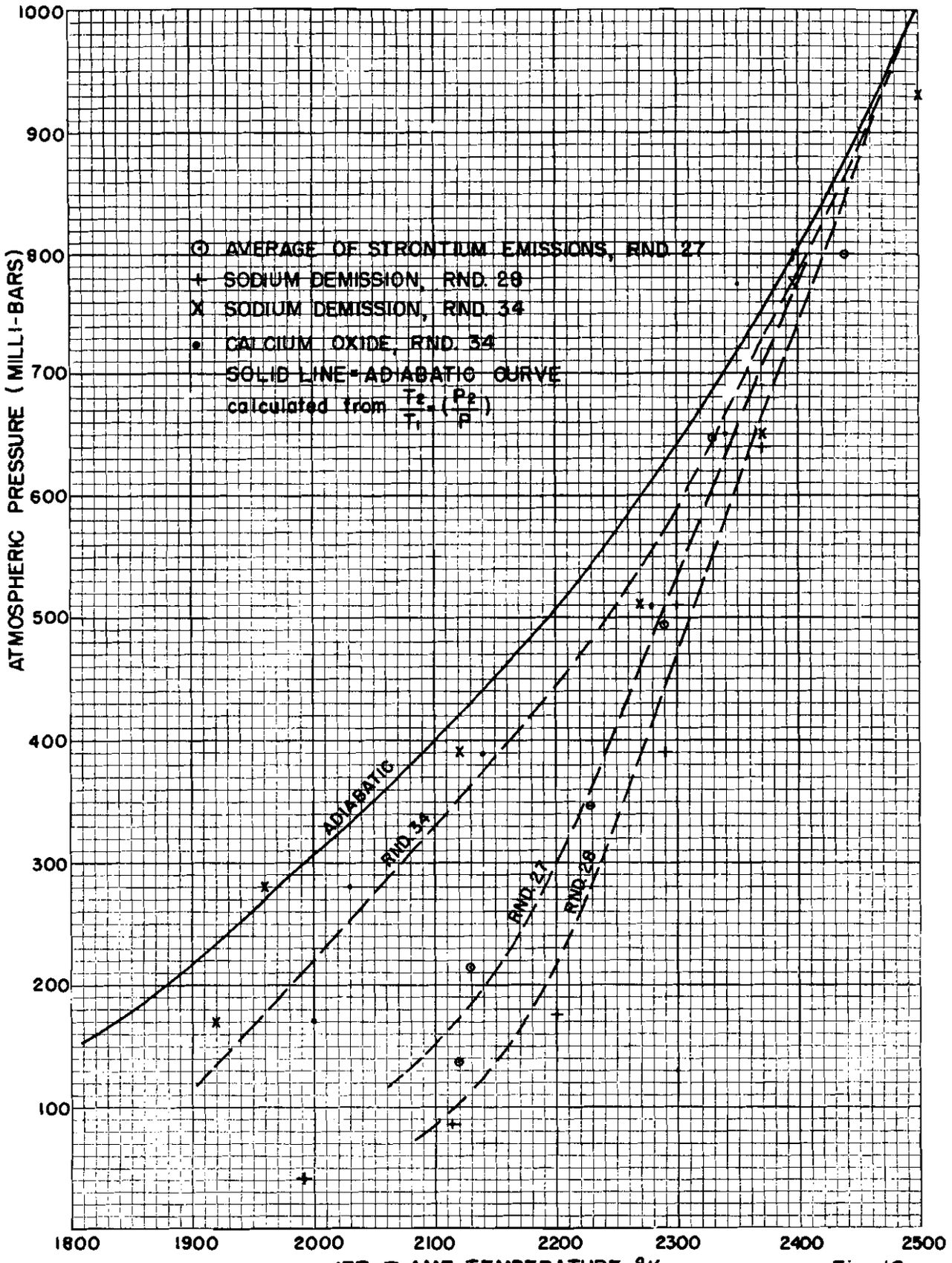
ATMOSPHERIC PRESSURE (MILLI-BARS)
1000
900
800
700
600
500
400
300
200
100
1800
1900
2000
2100
2200
2300
2400
2500
JET FLAME TEMPERATURE °K
⊙ AVERAGE OF STRONTIUM EMISSIONS, RND. 27
+ SODIUM DEMISSION, RND. 28
X SODIUM DEMISSION, RND. 34
• CALCIUM OXIDE, RND. 34
SOLID LINE = ADIABATIC CURVE
calculated from $\frac{T_2}{T_1} = \left(\frac{P_2}{P}\right)$
ADIABATIC
RND. 34
RND. 27
RND. 28

Fig. 10

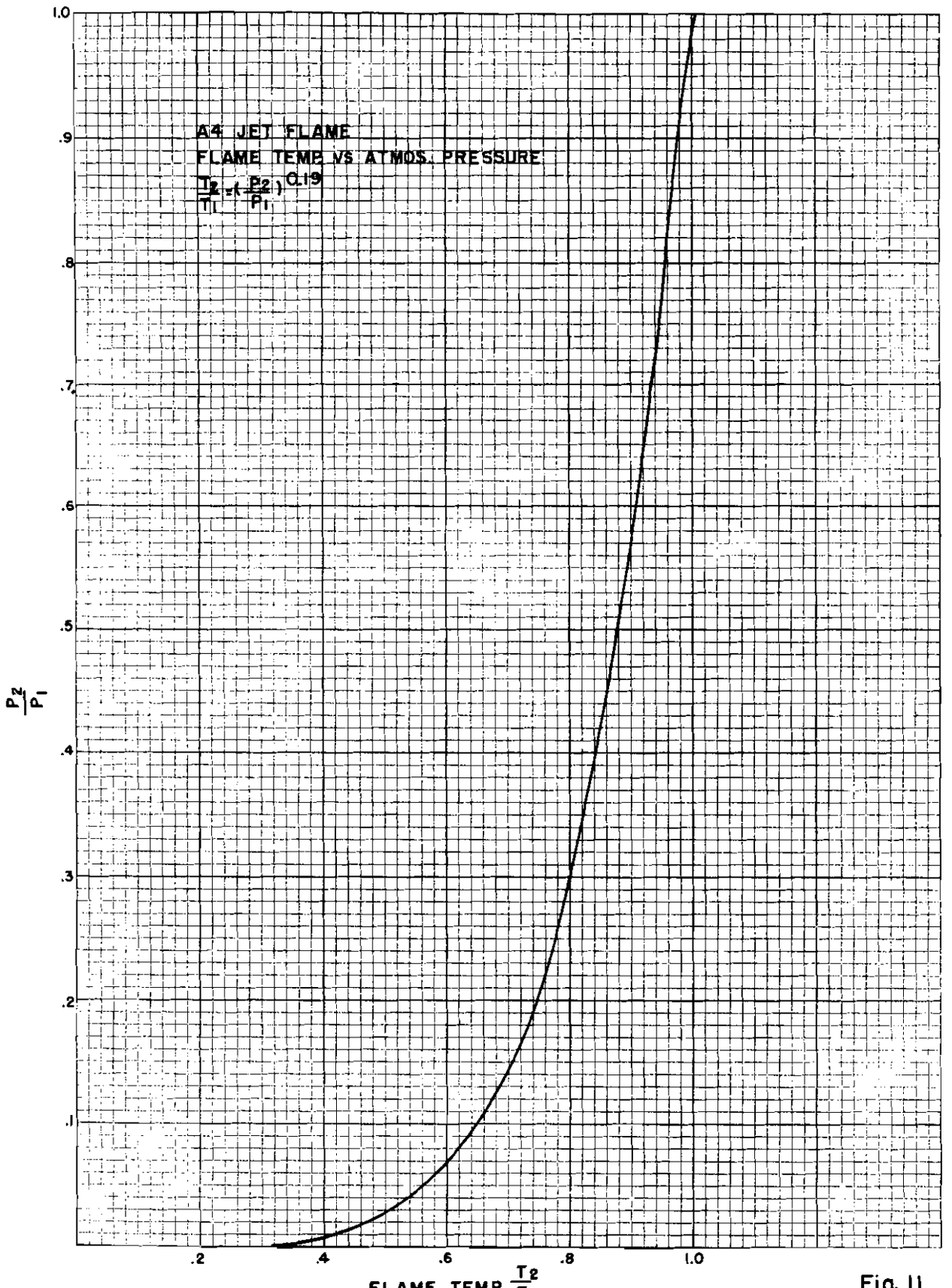
A4 JET FLAME
FLAME TEMP. VS ATMOS. PRESSURE
$\frac{T_2}{T_1} = (\frac{P_2}{P_1})^{0.19}$
1.0
.9
.8
.7
.6
.5
.4
.3
.2
.1
$\frac{P_2}{P_1}$
.2
.4
.6
.8
1.0
FLAME TEMP. $\frac{T_2}{T_1}$

Fig. 11

If this assumption is true then the jet density is inversely proportional to the jet cross section (or, approximately, to the square of the jet diameter). Thru this and the adiabatic assumption, we arrive at the relation:

$$\frac{T_2}{T_1} = \left(\frac{D_1}{D_2}\right)^{2(K-1)}$$

Where $\frac{T_2}{T_1}$ is the jet temperature ratio as before, and $\frac{D_1}{D_2}$ is the ratio of jet diameters for corresponding temperatures. K is the ratio fo specific heats of the jet gases.

We now prepare a chart (Figure 12), with $\frac{T_2}{T_1}$ and $\frac{D_2}{D_1}$ as arguments and plot the above relation as a family of curves for various K values. We note in passing that, from the probably chemical composition of the jet gases the expected value of K is about 1.24 Turning to the observational material, we average the corresponding pairs of values for $\frac{T_2}{T_1}$ and $\frac{D_2}{D_1}$ for Rounds 27 and 28. These observational results are plotted on Figure 13 and correspond to a K value of about 1.10 making C_p = 21 approximately twice the anticipated value. If this result is valid, it must mean that the jet gases contain a large and totally unexpected source of heat energy. If the result is not valid, we may, among other things, suspect the presence of non-thermal sources of jet emissions in the visible spectrum.

5. Summary of the Flame Temperature and Diameter Studies

We find that:

a. The measured jet cross section agrees with the assumptions of adiabatic expansion and jet pressure equal to ambient atmospheric pressure during the first 45 seconds of rocket flight, corresponding to altitudes up to about 50,000 ft.

b. Above 50,000 feet the jet cross section curve departs increasingly from the "adiabatic-atmospheric" curve, the jet cross section being smaller than these assumptions require. This suggests that either the pressure on the jet surface is greater than the ambient atmospheric, or the pressure fall in the expanding jet is greater than the adiabatic.

c. Jet temperatures based on spectrophotometry are higher than the corresponding temperatures calculated on an "adiabatic atmospheric" assumption, especially in Rounds 27 and 28, and, to a small extent, in Round 34. This checks qualitatively with (b) above, and suggests that the assumption of jet pressure equal to ambient atmospheric pressure is of limited validity.

d. Comparison of spectrographically estimated jet temperatures and measured jet diameters with the aid of an adiabatic relation and the assumption of constant axial jet velocity leads to a value of $K \approx 1.10$ for the average of Rounds 27 and 28. Round 34 gives $K \approx 1.15$, nearer to the expected value of $K = 1.24$. These results indicate that the jet radiates more than the expected amount of light for a given jet cross section.

We may assume that one or more of the following hypotheses will explain the excess radiation.

(1) The jet temperature is actually higher than adiabatic behavior with K = 1.24 would indicate. This would imply that either C_p is considerably higher than anticipated, or there

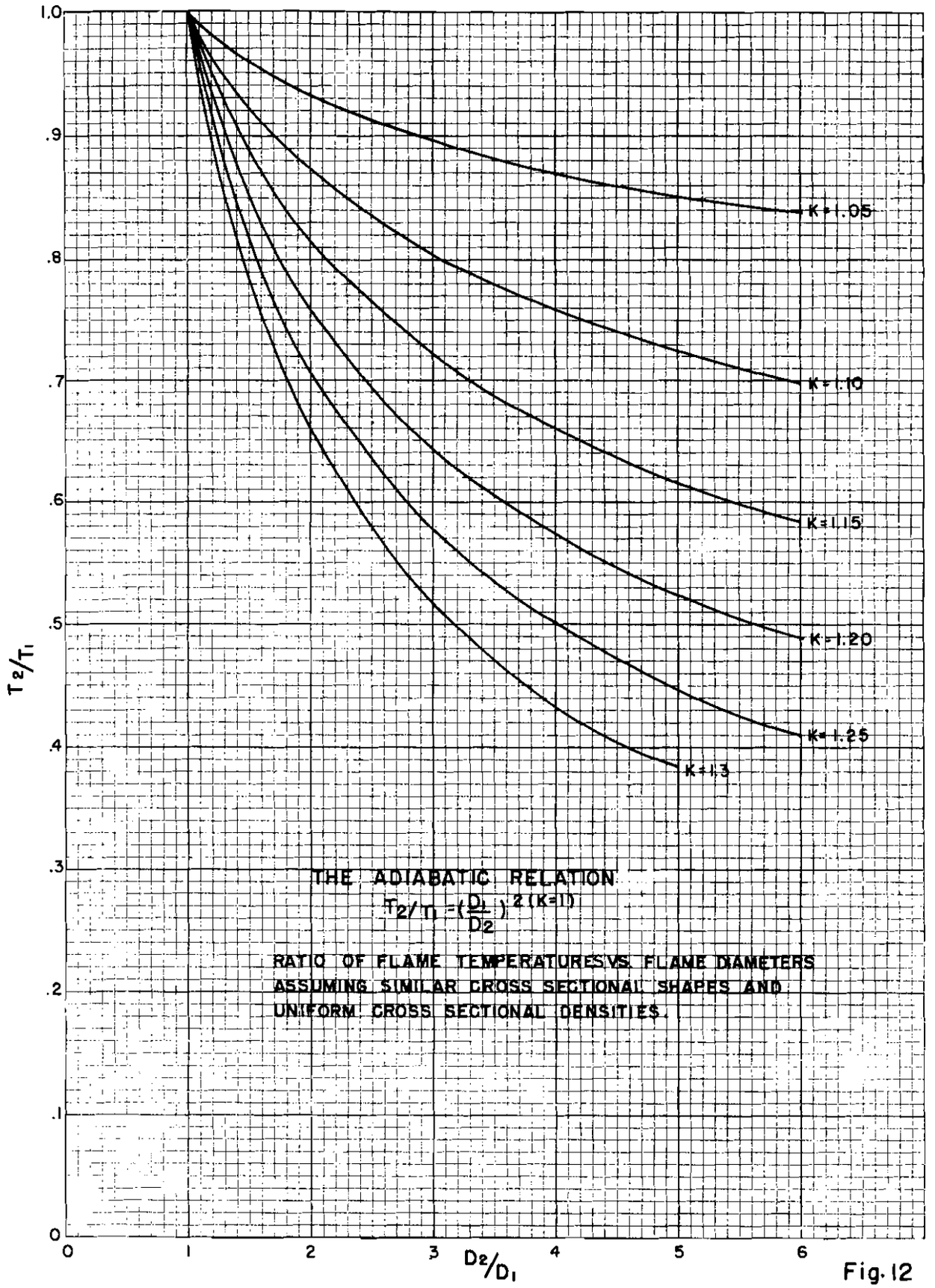
1.0
.9
.8
.7
.6
.5
.4
.3
.2
.1
0
T_2/T_1
K=1.05
K=1.10
K=1.15
K=1.20
K=1.25
K=1.3
THE ADIABATIC RELATION
$T_{2/T_1} = (\frac{D_1}{D_2})^{2(K-1)}$
RATIO OF FLAME TEMPERATURES VS. FLAME DIAMETERS
ASSUMING SIMILAR CROSS SECTIONAL SHAPES AND
UNIFORM CROSS SECTIONAL DENSITIES.
0
1
2
3
4
5
6
D_2/D_1

Fig. 12

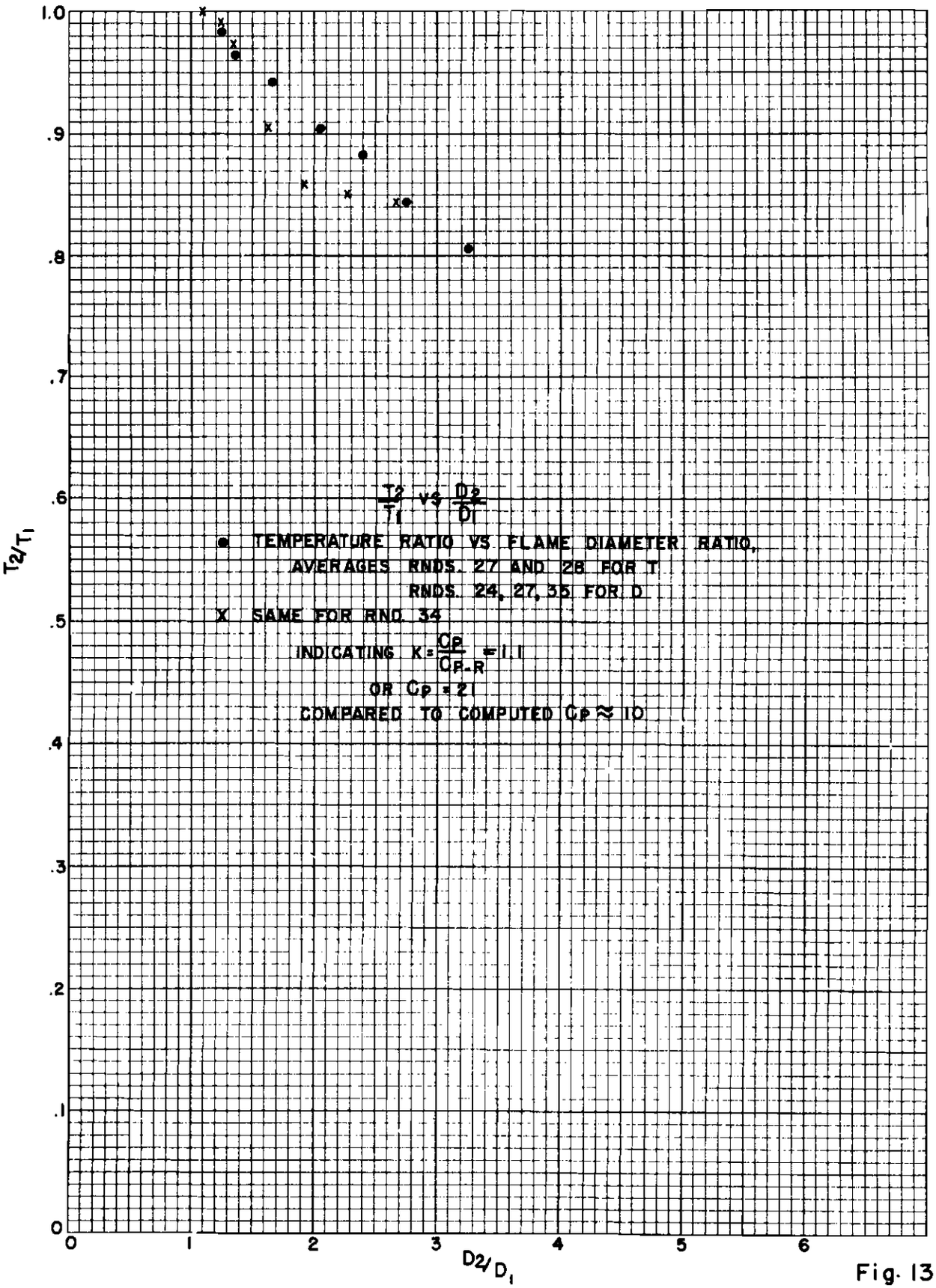
1.0
.9
.8
.7
.6
.5
.4
.3
.2
.1
0
T_2/T_1
0
1
2
3
4
5
6
D_2/D_1
$\frac{T_2}{T_1}$ VS $\frac{D_2}{D_1}$
● TEMPERATURE RATIO VS FLAME DIAMETER RATIO,
AVERAGES RNDS. 27 AND 28 FOR T
RNDS. 24, 27, 35 FOR D
X SAME FOR RND. 34
INDICATING $K=\frac{C_P}{C_P-R}=1.1$
OR $C_P=21$
COMPARED TO COMPUTED $C_P \approx 10$

Fig. 13

are heat sources in the jet. One such heat source is the burning of oxygen from the turbine exhausts with the alcohol-rich jet surface. However, the heat available from this reaction would not seem sufficient to account for the observed result.

(2) Part of the visible jet radiation is excited by other than thermal processes. It is known that the jet is sufficiently ionized to affect the propagation of radio waves. German conductivity measurements with probes have confirmed the existence of considerable ionization in rocket flames. Perhaps in some way the free electrons associated with this ionization are acted upon by sufficiently strong fields so that in the upper atmosphere, they excite visible radiation within the jet. During the time involved in these observations, the missile moves thru the vertical electrical gradient of the atmosphere at a rate of thousands of volts per second.

(3) The shock thrown across the jet by collision between the jet and the supersonic air stream may become increasingly intense as the missile rises, with a corresponding decrease in axial jet velocity and increase in jet density. This would invalidate the assumption of constant axial jet velocity and lead to an observed jet brightness greater than that predicted by by the theory employed above. Measurements and aerodynamic interpretations of the jet structure so far made do not seem to indicate a large effect of this kind.

VII. AERODYNAMICS OF THE JET FLAME OF THE A4 MISSILE FLYING AT SUPERSONIC VELOCITIES.

A. The Sonic Transition.

The disappearance of the Mach nodes from the flame as the missile passes through sonic velocity can be understood in terms of the pressure distribution in the atmosphere on the exterior surface of the jet. When the missile is stationary, as in a static firing, this pressure is everywhere constant and we have the classic case treated by Mach and others. If the missile moves, the Mach pattern and the "wavy wall" of the jet boundary associated with the periodic rarefactions and condensations within the jet move thru the atmosphere with the missile. The flow of air along the wavy jet wall now causes variations in the external pressure on the jet from point to point. So long as the missile (and the Mach pattern) move thru the air at subsonic velocities, these external pressure variations tend to accentuate rather than destroy the waviness of the jet wall associated with the Mach nodes. (See Figure 14a). The nodes therefore persist. As the missile reaches the transonic velocity range, regions of supersonic flow appear first on the outward "bulges" of the wavy wall (see Figure 14b). The resultant intense disturbances of the jet wall are visible in motion pictures of the jet taken with a missile-borne camera, by the Naval Research Laboratory and also on tracking telescope records. These destroy the train of Mach nodes by "roughening" of the walls of the jet so that the orderly reflection of disturbances within the jet no longer takes place.

In a short time, the missile accelerates to definitely supersonic velocities, and the jet bourdary resumes its smooth appearance. However, the train of Mach nodes cannot reform at supersonic velocities. The nature of the external pressure pattern caused by "waves" or "corners" in the jet surface tends to erase these irregularities and to carry away thru the boundaries of the jet some of the momentum from the internal jet expansions and compressions causing them. The "total reflection" property of the jet walls which makes possible the multiple reflections associated with the Mach node train is destroyed.

Figure 14c outlines the situation in which a shock wave meets the wall of the jet flame past which air is flowing at supersonic velocity. The shock wave deflects the direction of flow. But the angle of deflection is reduced by the fact that a shock springs from the corner thus formed into the air outside the jet. The air pressure behind this shock is increased, and the expansion angle of the jet wall corresponds to this increased external pressure. Similarly, expansions and compressions in general are partly transmitted, partly reflected at the jet wall.

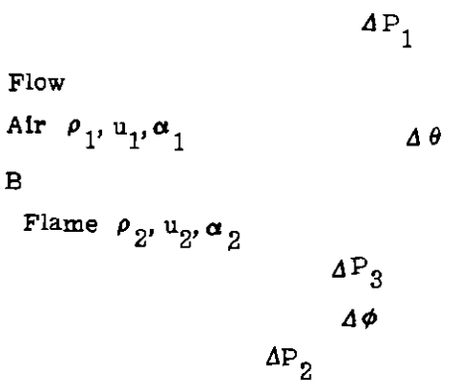

Consider the situation in a small region surrounding the intersection of a weak compression (or expansion) with the jet boundary B while the missile is flying at a supersonic velocity. From linearized flow theory (11) we have

$$\Delta P_2 = \rho_2 u_2^2 \tan \alpha_2 \quad \Delta\phi$$

$$\Delta P_1 = \rho_1 u_1^2 \tan \alpha_1 \quad \Delta\theta$$

And for the reflected pressure change

$$\Delta P_1 = \Delta P_2 - \Delta P_3$$

$$\Delta P_3 = \rho_2 u_2^2 \tan\alpha_2 \left(\Delta\phi - \Delta\theta\right)$$

So: $$\rho_1 u_1^2 \tan\alpha_1 \quad \Delta\theta = \rho_2 u_2^2 \tan\alpha_2 \left(2\ \Delta\phi - \Delta\theta\right)$$

or: $$\frac{\Delta\theta}{\Delta\phi} = \frac{2\ \rho_2 u_2^2 \tan \alpha_2}{\rho_1 u_1^2 \tan \alpha_1 + \rho_2 u_2^2 \tan \alpha_2}$$

Or: $$\frac{\Delta\phi}{\Delta\theta} = 1/2\left(1 + \frac{\rho_1 u_1^2 \tan \alpha_1}{\rho_2 u_2^2 \tan\alpha_2} \right)$$

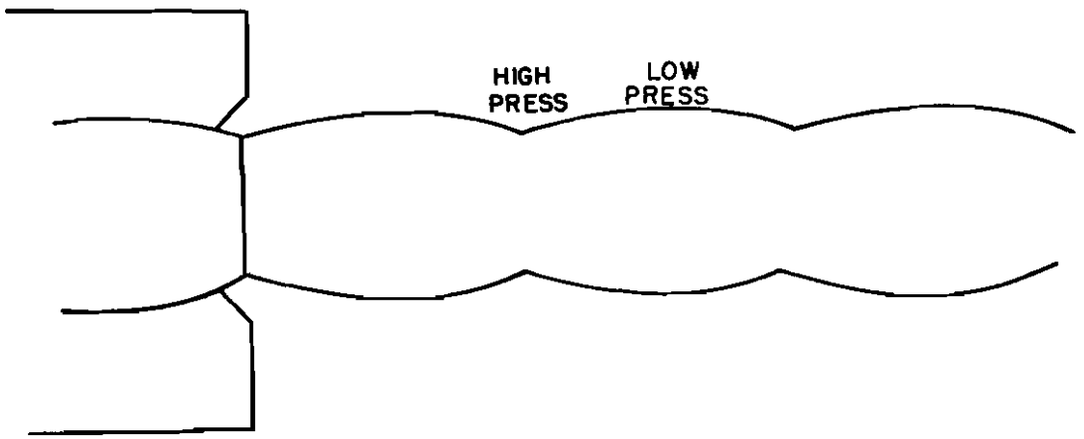

A) SUBSONIC MISSILE VELOCITY
MACH NODES PERSIST

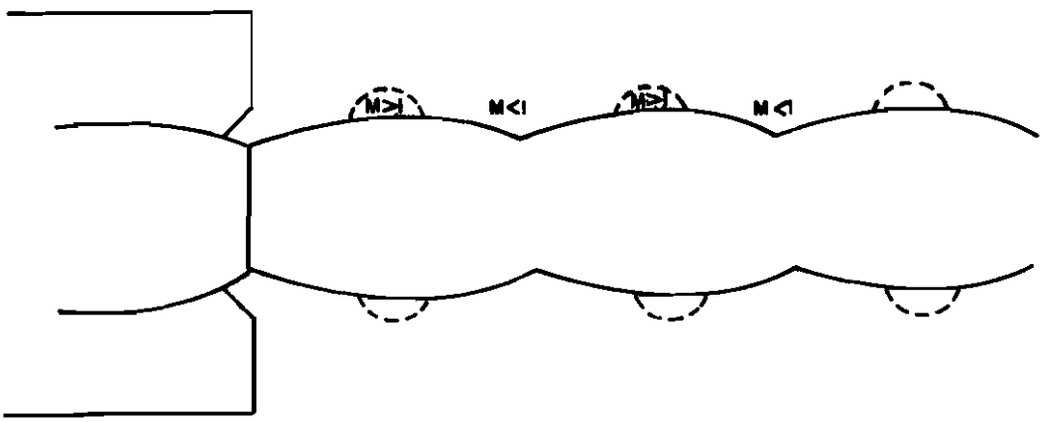

TRANSONIC MISSILE VELOCITY
MACH NODES DESTROY THEMSELVES
BY CREATING UNSTABLE SURFACE

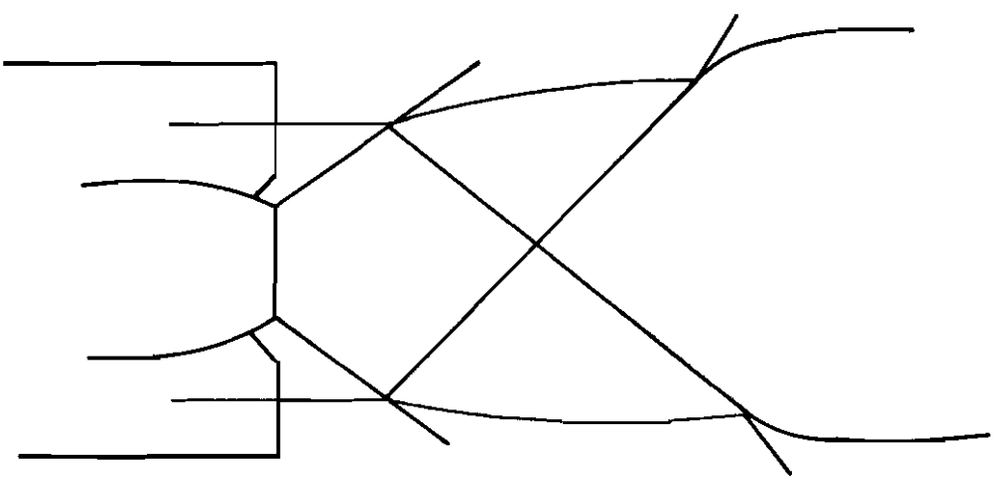

SUPERSONIC MISSILE VELOCITY
JET WALL REFLECTIVITY < 1

FIG. 14

For the "reflectivity" of the jet wall with respect to distubrances impinging upon it from within the jet we have:

$$R = \frac{\Delta P_3}{\Delta P_2} = \frac{\Delta\phi - \Delta\theta}{\Delta\phi} = 1 - \frac{\Delta\theta}{\Delta\phi}$$

In Figure 15 this reflectivity is plotted against missile Mach number for the A4 jet flame, using the approximations listed there. It is seen that the conditions for formation of the Mach node train are destroyed at the instant of sonic transition, never to return. This must be generally true of all jet-bearing missiles travelling at supersonic velocities thru the atmosphere. The partial reflection of disturbances from the jet wall at missile Mach 1.1 to 3 can and does produce one or two cycles of jet distrubance in the A4 flame, but these are excited by the encounter of the jet with the supersonic air stream around the missile, not by the expansion or contraction of the jet upon leaving the nozzle orifice as in the case of the Mach nodes.

B. Efflux Angle of the Jet Flame Boundary.

As the jet emerges from the nozzle orifice into a region of reduced pressure in the subsonic turbulent boundary layer around the missile, the jet surface is deflected thru such an angle as to make the pressure continuous across the surface. Observation shows that just after the missile passes sonic velocity this turbulent layer is only a few inches thick at the stern of the A4 missile. This thickness increases to a foot or more as the missile approaches a speed of one mile per second and an altitude of twenty miles at propulsion cutoff. When the jet surface meets this boundary layer it turns thru an angle $\Delta\theta_1$, (Figure 16) in order that:

$$\Delta P_{f_1} = P_f - P_t = \rho_f u_f^2 \tan \alpha_f \ \Delta\theta_1,$$

The pressure P_t in the turbulent layer can be calculated approximately from P_a of the undisturbed air flow and the angle which the outer boundary of the turbulence makes with the original flow axis. This angle is observed to be always less than the 'boattail' angle of the missile skin with the missile axis at the stern of the A4 missile, and near propulsion cutoff is such as to divert the airflow slightly outward, corresponding to a pressure greater than P_a.

The jet surface then continues outward and to the rear with a slight rearward curvature until it approaches the supersonic air stream along the outer limit of the turbulent layer. At this point a pair of shocks or at least very rapid compressions are generated, one inside the jet and one in the air outside. The two flows are still separated by a thin sheet fed between them from the turbulent layer. The jet boundary curves rapidly rearward for a short distance near this point, then becomes almost straight again. The situation in this vicinity requires the pressure jumps just inside and outside the jet surface to be equal:

$$\Delta P_a = \Delta P_{f_2}$$

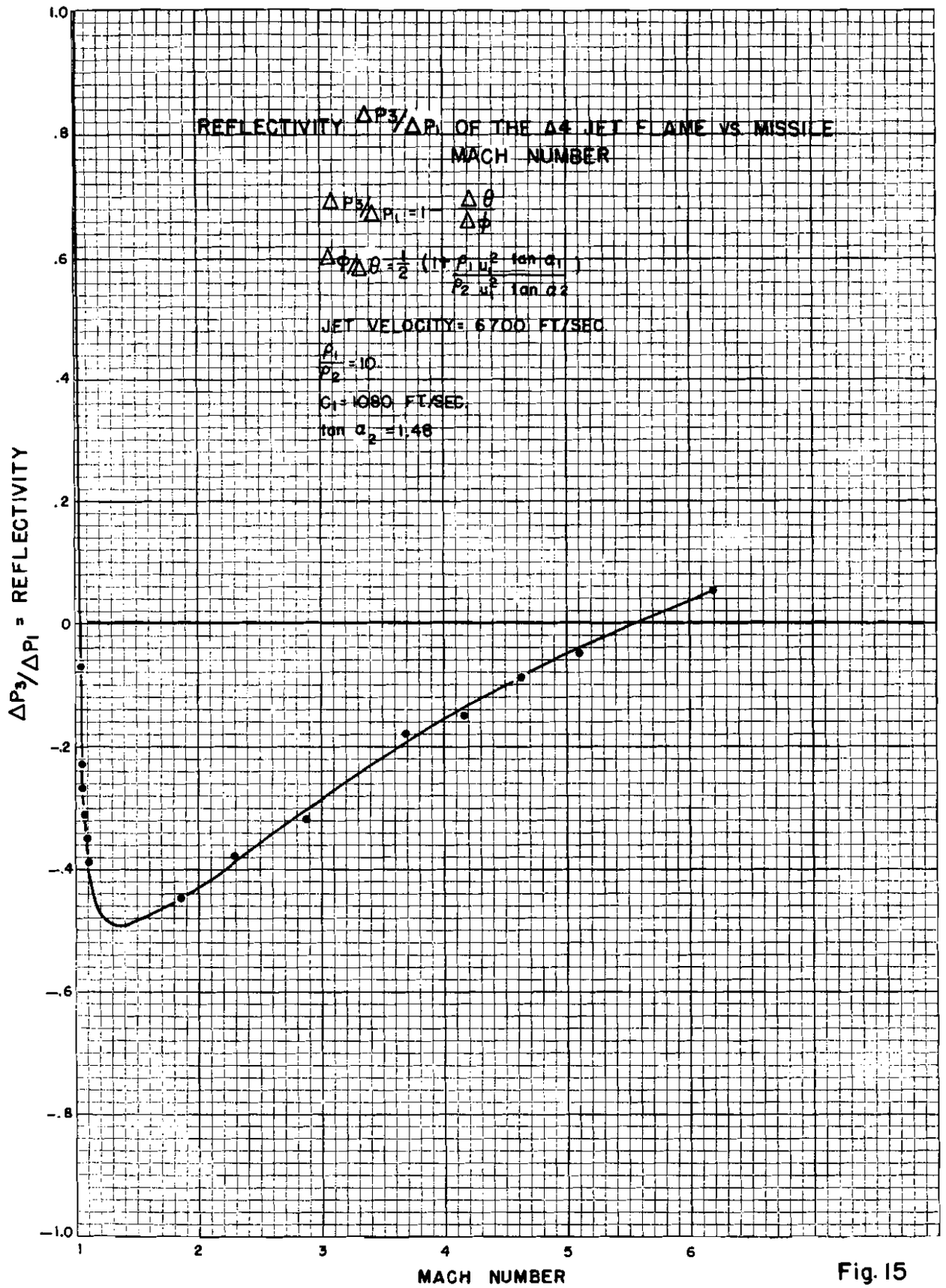
REFLECTIVITY $\Delta P_3/\Delta P_1$ OF THE A4 JET FLAME VS MISSILE MACH NUMBER
$\Delta P_3/\Delta P_1 = 1 - \frac{\Delta\theta}{\Delta\phi}$
$\Delta\phi/\Delta\theta = \frac{1}{2}\left(1 + \frac{\rho_1 u_1^2 \tan\alpha_1}{p_2 u_1^2 \tan\alpha_2}\right)$
JET VELOCITY = 6700 FT/SEC.
$\frac{\rho_1}{\rho_2} = 10.$
$C_1 = 1080$ FT/SEC.
$\tan\alpha_2 = 1.46$
$\Delta P_3/\Delta P_1$ = REFLECTIVITY
1.0
.8
.6
.4
.2
0
-.2
-.4
-.6
-.8
-1.0
1
2
3
4
5
6
MACH NUMBER

Fig. 15

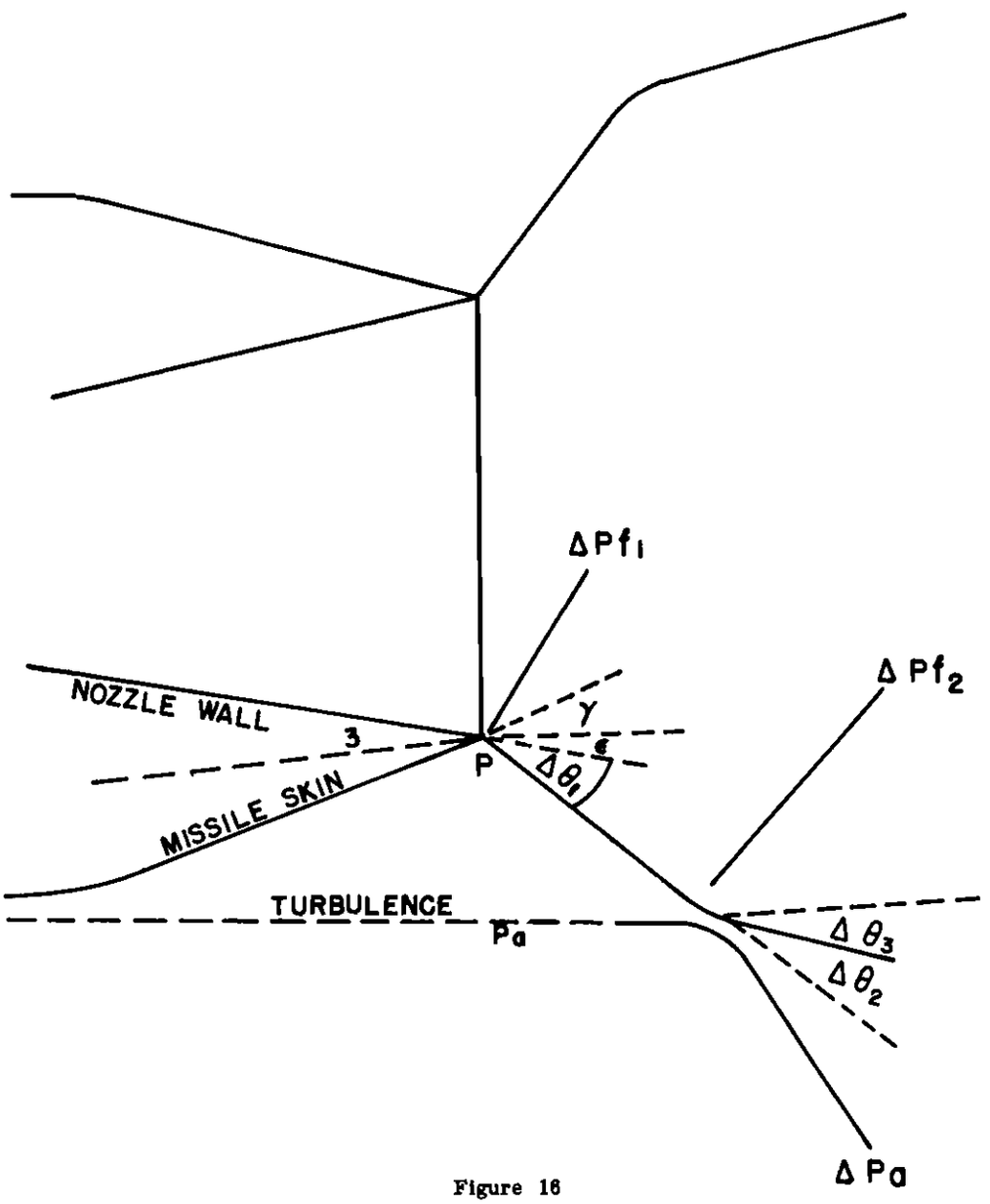

Figure 16

And in the neighborhood of this point we have approximately:

$$\Delta P_a = \rho_a u_a^2 \tan \alpha_a \ \Delta\theta_3$$

$$\Delta P_{f_2} = \rho_{f_2} u_{f_2}^2 \tan \alpha_{f_2} \ \Delta\theta_2$$

$$\Delta\theta_1 + \epsilon - \Delta\theta_2 = \Delta\theta_3$$

From these it follows that

$$\frac{\Delta\theta_1 + \epsilon}{\Delta\theta_2} = \frac{\Delta\theta_3}{\Delta\theta_2} + 1 = 1 + \rho_{f_2} u_{f_2}^2 \tan \alpha_{f_2}$$

Here the known or measurable quantities are $\Delta\theta_1$, $\Delta\theta_2$, $\Delta\theta_3$, ϵ, and $\rho_a u_a^2 \tan \alpha_a$. Hence it is possible to calculate ΔP_a, ΔP_{f_2}, and $\rho_{f_2} u_{f_2}^2 \tan \alpha_{f_2}$.

The internal compression thus generated crosses the jet and meets the opposite boundary. The situation in the neighborhood of the resultant boundary deflection can be described with the aid of the boundary reflection relations given in the section of sonic transition.

C. Bilateral Symmetry of the Jet.

Intuition makes easy the acceptance of the idea that a jet expanding out of an axially symmetric rocket motor in an axially symmetric missile flying with no yaw will be itself axially symmetrical. Therefore the discovery of a pronounced axial asymmetry of the A4 jet flame came as a surprise. The bilateral symmetry of the observed pattern led to a search for bilaterally symmetric features in the structure of the missile. Only one was found, namely the two fuel pump turbine steam exhausts midway between pairs of fins on opposite sides of the missile near the rear end of the missile body. Tracking telescope records disclosed that the broad, bright wings of the jet appear always under these two exhausts. When a missile loses roll control and rotates, the winged pattern rotates with it, maintaining alignment with these vents.

The causal connection between the exhaust vents and the flame pattern seems thus sufficiently well established. The question how a total of 250 lbs. of turbine exhaust gases, emitted at subsonic velocity, can so greatly affect 9 tons of jet gases emitted with a velocity of 6700 feet per second, now invites an answer. The basis for that answer will be furnished in the form of a more detailed examination of the jet structure, the turbulent boundary layer around the missile, and the reaction of free oxygen in the turbine gases with the alcohol-rich surface of the jet. Plates 2A and 2B, taken by Tracking Telescopes 1 and 2 respectively, show A4 Round 27 as viewed in two approximately perpendicular vertical planes. It happens that Telescope 1 views the missile nearly along the 'minor' flame plane, and thus sees the broad aspect of the flame. Telescope 2 sees the 'narrow' flame aspect.

Round 27 was chosen for this example because the addition of strontium brightened the flame without disturbing the flame pattern. This makes easily visible the outlying parts of the flame as seen from the narrow viewpoint, which are normally so faint as to be difficult to see. Information from this and other rounds is incorporated in Figure 17 showing the two aspects of the flame and the corresponding cross sections at various points along the flame axis at about 50 seconds after missile takeoff.

It is seen that the ovalness is principally due to variations in the thickness of the turbulent layer, the major axis of the oval lying under the turbine exhausts, one of whose effects is now seen to be the thickening of the boundary layer by adding low velocity material to it, thus increasing its volume and decreasing its velocity. The jet thus continues to expand to a greater radius before being shocked back by the supersonic air stream. At the same time, the boundary layer is markedly thinner in a plane containing the missile axis and the 'minor axis' of the jet. Correspondingly, the expansion angle of the jet is cut back by al-

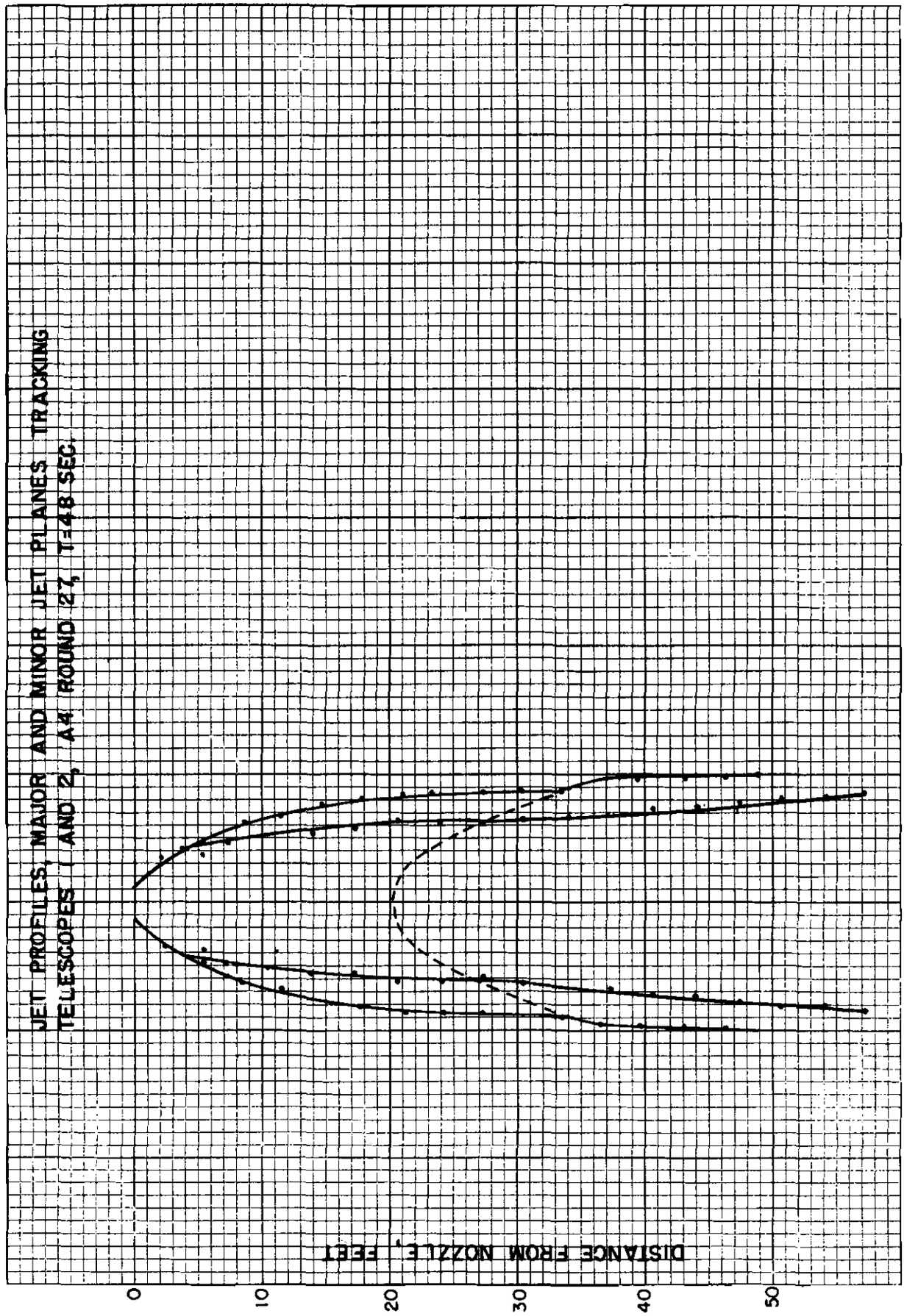
JET PROFILES, MAJOR AND MINOR JET PLANES TRACKING
TELESCOPES 1 AND 2, A4 ROUND 27, T=48 SEC.
DISTANCE FROM NOZZLE, FEET
0
10
20
30
40
50
DISTANCE FROM JET AXIS, FEET
20
10
0
10
20

Fig. 17

most immediate encounter with the supersonic air stream after emerging from the nozzle, so the jet radius remains smaller in this plane for some distance back of the nozzle orifice. Only after being 'shocked out' again by the compression emanating from the normal shock formed in the jet as shown in the photographs does this surface begin to expand at a sufficient rate to make the jet round.

Even after the ovalness of the jet begins to decrease the brightness distribution in the flame continues to give the appearance of a strongly flattened 'wing'. This is traceable to the fact that free oxygen in the turbine exhaust burns with the alcohol-rich surface of the jet flame. The combustion is seen to become suddenly quite intense at the point where the turbine exhaust gases are caught between the impinging jet and supersonic air stream, and elevates the temperature of the jet surface for twenty or thirty feet downstream sufficiently to brighten the surface appreciably. This combustion effect was pointed out by German scientific personnel in a conference on the subject at Ft. Bliss, Texas.

The turbine exhaust consists of the decomposition products of H_2O_2, which is catalyzed with sodium permanganate to form steam for the fuel pump turbine at a rate of about 4 pounds per second. Thus, roughly two pounds of oxygen is released per second, and from each of the two exhausts the oxygen flow rate is approximately one pound per second. The surface of the jet as it emerges from the rocket nozzle is rich in the unoxidized alcohol which is sprayed in thru holes in the nozzle wall to protect the wall from heat and oxidation. The pound of oxygen will mix with the jet surface to form a streak about two feet wide, a few inches thick, and several thousand feet long. The total amount of the jet material involved in the mixture is probably about 2000 cu. ft. with an estimated mass of the order of 7 Kg. The heat released by the pound of oxygen burning with alcohol is about 3500 Kg. cal. This is sufficient to brighten the jet surface and to cause a sudden diabatic pressure rise at the nozzle like 'opening' thru which the turbulent layer passes between the impinging jet and supersonic air stream. As a result of this combustion-generated pressure increment and its rapid decline as the thin layer containing it expands, a ray-like brightening passes diagonally across the body of the jet, contained between the combustion-generated compression wave and the expansion which follows it at a distance of a foot or so. The distinctness of this feature varies from round to round, but it can usually be seen between 30 and 40 seconds after takeoff, and frequently the bright cross it forms in the flame as viewed from Telescope 1 is one of the most striking features of the jet pattern. It seems very likely that this combustion process has a strong role in producing the increased thickness of the turbulent boundary layer observed underneath the steam exhaust ports. The intense burning of alcohol and oxygen at the point of collision of jet and airsteam builds up pressure and acts like a dynamic "plug", raising the pressure in the "lake" of turbulent flow above it.

Not only is the depth of the "lake" correspondingly increased, but the pressure rise produces a component of thrust on the boat-tail of the missile. We thus have the spectacle of the A4 missile propelled thru the upper atmosphere by a force produced in part by combustion in the gas flow outside of, and indeed at a distance of several feet from the missile.

D. Stability of an Expanding Jet of Oval Cross Section.

For a jet whose walls are everywhere parallel to the direction of flow of the undisturbed supersonic air stream around it, the wall pressure is everywhere constant regardless of the shape of the jet cross section. However, if the jet wall at any place diverges or converges with respect to the flow axis, (or if the

jet contains compressions or expansions, which comes to the same thing) the jet cross section will not in general be stable; that is, the pressure of the external air flow will vary from point to point around the periphery of the cross section and this will lead to changes in the cross sectional form at downstream points. Consider as a simple model a wedge capped on each end by a half-cone, flying without yaw at supersonic velocity (Fig. 18a). On the wedge, the pressure increment is approximately:

$$\Delta P_w = \rho u^2 \tan \alpha \, \Delta\theta$$

On the cone, the approximation is:

$$\Delta P_c = \rho u^2 \log \left(\frac{1}{\Delta\theta}\right) \Delta\theta^2$$

The equilibrium condition is:

$$\Delta P_w = \Delta P_c$$

Or:

$$\Delta\theta \log \left(\frac{1}{\Delta\theta}\right) = \tan \alpha$$

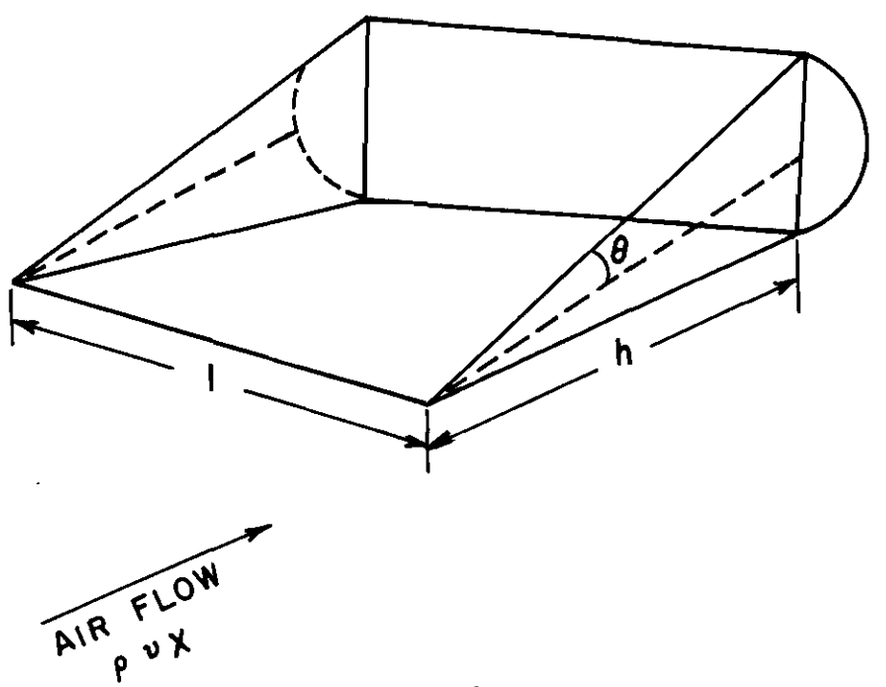

Figure 18a

This relation is plotted in Figure 18b which displays the areas in which $\Delta P_w > \Delta P_c$ below and to the left of the curve, while the region of $\Delta P_w < \Delta P_c$ lies above and to the right. Reference to Figure 17 shows that the jet near the nozzle approximates a cone. Figure 18b indicates that in contact with the axially symmetrical air stream the conical jet will in many circumstances be unstable. Consider a perturbation which destroys over a small strip the curvature of the jet cone. Over this wedge-like strip an increased pressure can appear and this in turn will enhance the effect of the disturbance so that downstream the jet surface will not regain its former conical outline and may indeed depart increasingly from it. In the case of the A4 jet, the asymmetry of the turbulent boundary approximates the proper type of perturbation and the expanding cone is probably unstable up to about missile Mach 2.5, which is reached about 45 sec. after takeoff. This probably enhances the effect of the jet distorting factors

E. Missile Design Considerations Derived from the Jet Flame Study.

German wind tunnel experiments (3) have shown that the jet flame has an important effect on missile drag. The drag coefficient was observed to increase by as much as 75% at low subsonic velocities and to decrease by as much as 18% at supersonic velocities when the jet was turned on. At sonic missile velocity, the drag is substantially unaffected by the jet. The German workers conclude that the effect of the jet on missile drag is due to jet-induced pressure changes on the boattail stern of the missile. At subsonic missile velocities the jet exerts an 'aspirator' effect, entraining air in its boundary and accelerating the flow of air around the bottail, causing a pressure drop there. This causes an increase in drag. At supersonic missile velocities the presence of the expanding jet cone is observed to increase the thickness of the turbulent layer over the boattail. The supersonic flow, which controls the effective pressure on the boattail under these circumstances, is deflected thru less than the boattail angle or even diverges from the missile axis. The corresponding increase in boattail pressure decreases the drag, or can even add a net thrust when the supersonic flow diverges from the flow axis, as is at times the case for flow around the V-2 in the plane of the steam exhausts.

This accidental creation of thrust by such a novel mechanism invites the question whether the effect can be enhanced by deliberate design. Three elements are necessary: (1) a jet surface of supersonic flow diverging sharply from the stern of the missile; (2) a missile surface so shaped that the pressure developed in the diverging supersonic air flow around the missile and transmitted thru the turbulent layer will deliver a thrust component of force, (3) an adequate supply of air or other material to build up the turbulent layer to the necessary thickness. A fourth desideratum is the presence of a flame "plug" where jet and supersonic air stream collide. The problem presented is a complicated one which would probably require the establishment of some parameters by experiment, but the large observed effect on the A4 boundary layer produced by the addition of four pounds per second of turbine exhaust gas indicates the desirability of further work.

The possibility of obtaining somewhat more thrust than is at present derived from the A4 rocket is dramatically displayed by the spectacle of the gigantic jet, more than twenty feet in diameter and equivalent to a solid body of the same form, driving its way thru the high atmosphere at velocities of 3000 ft/sec. or more. This it can do by the thrust it generates in expanding after leaving the rocket nozzle. The thrust is created by reaction against the 'nozzle' of the atmospheric surface around the jet. This nozzle can be-

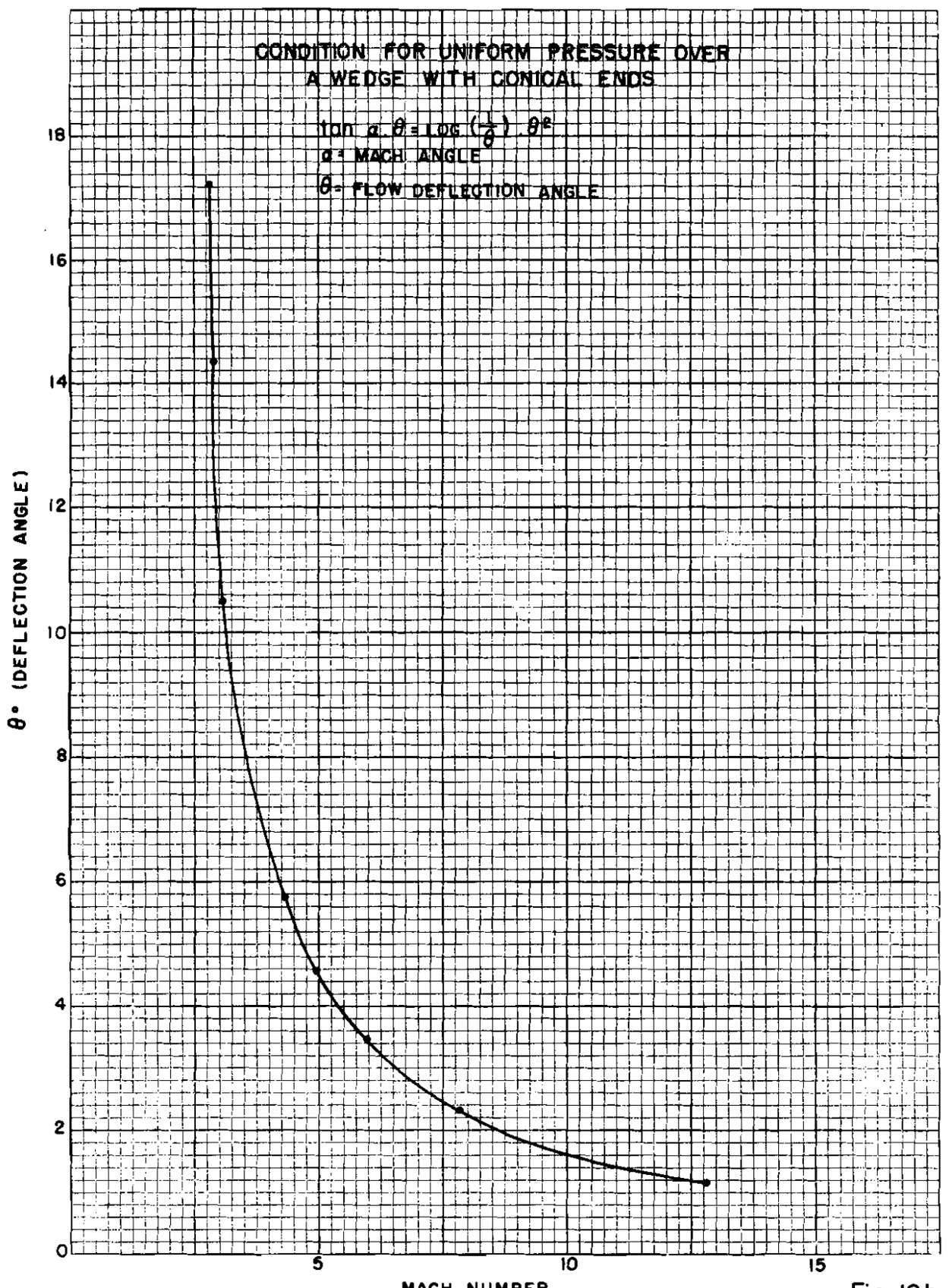
CONDITION FOR UNIFORM PRESSURE OVER A WEDGE WITH CONICAL ENDS
$\tan \alpha . \theta = \log\left(\frac{1}{\theta}\right) . \theta^2$
α = MACH ANGLE
θ = FLOW DEFLECTION ANGLE
$\theta°$ (DEFLECTION ANGLE)
0
2
4
6
8
10
12
14
16
18
5
10
15
MACH NUMBER

Fig. 18b

come almost perfectly efficient, since reference to Figure 11 shows that the reflectivity of the jet boundary becomes very small at higher missile velocities. Under these conditions, each expansion ray is 'extinguished' at the jet boundary and a uniform source at the rocket exit will result in parallel flow in the airy 'nozzle' with the ultimate extinction of all disturbances and the delivery of maximum 'jet velocity'.

The observation of the elliptical cross section of the A4 jet and the recognition of the connection between cross sectional shape and surface pressure led to the question whether an axially symmetrical missile body is best with respect to drag. In this matter once again the wedge and the cone offer simple models for comparison. Consider a cone and a wedge whose bases have the same area K and altitude h. The drag on the wedge is approximately

$$D_w = \frac{1}{hl} k^2 \rho u^2 \tan\alpha$$

where l is the wedge length parallel to the leading edge.
The drag on the cone is approximately

$$D_c = \frac{\text{Log}\left(\sqrt{\frac{\Pi}{k}}\, h\right)}{h^2} \quad \frac{k^2 \rho u^2}{\Pi}$$

For $D_c = D_w$ we have

$$\frac{\text{Log}\sqrt{\frac{\Pi}{k}} + \text{Log}\, h}{\Pi h} = \frac{\tan\alpha}{l}$$

Or:

$$l = \frac{\Pi h \tan\alpha}{\text{Log}\sqrt{\frac{\Pi}{k}} + \text{Log}\, h}$$

the wedge length at which wedge drag is equal to cone drag.

A wedge length greater than l will give a wedge drag less than that of a cone of the same height. A wedge of length 2l will have half the drag of the comparable cone. To simplify computation, let the base area $K = \Pi$ and $\tan\alpha = 1/2$
Then:

$$l = \Pi \tan\alpha \frac{h}{\text{Log}\, h} \quad \text{and} \quad \Pi \tan\alpha = 1.57$$

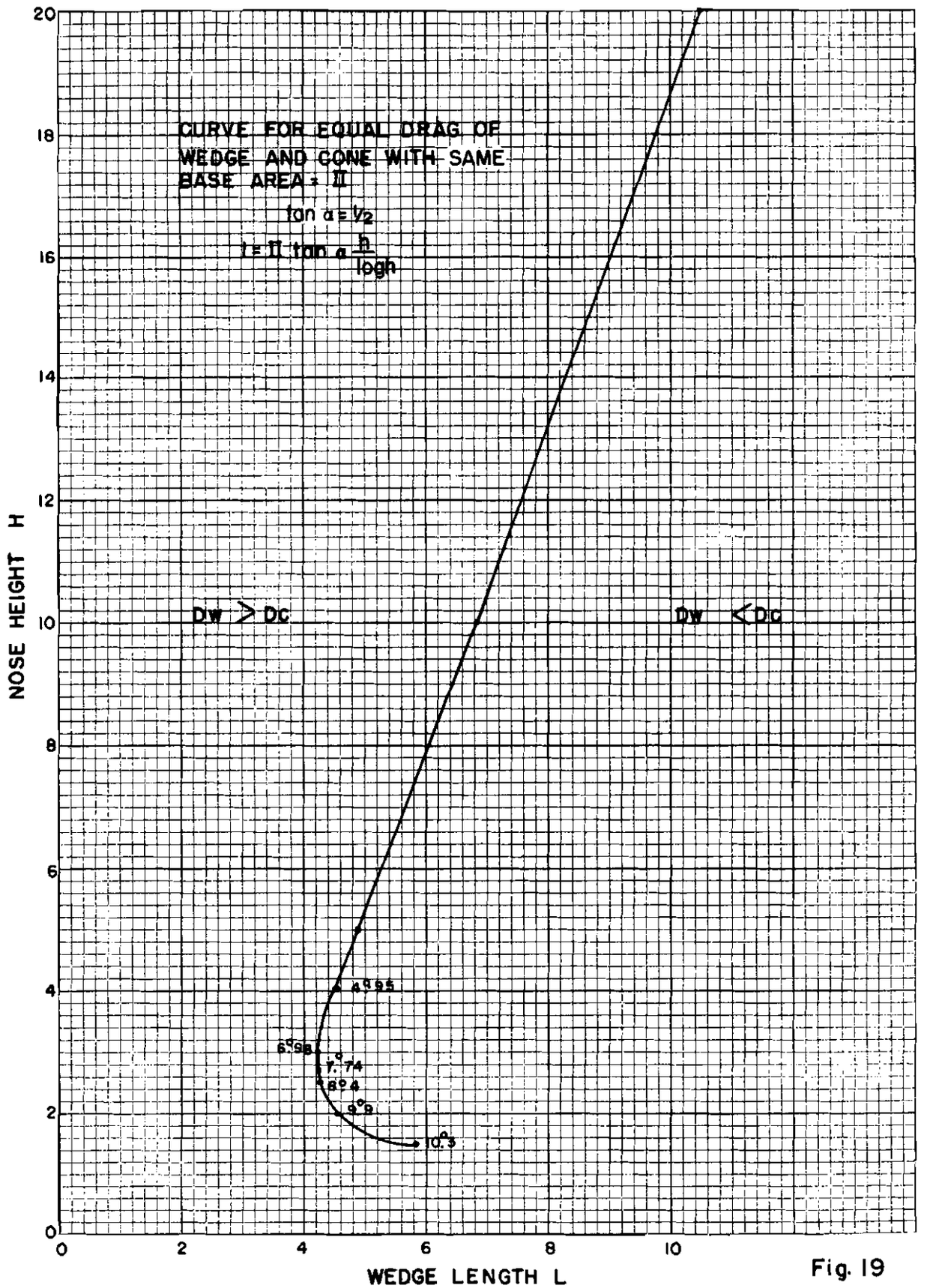
CURVE FOR EQUAL DRAG OF WEDGE AND CONE WITH SAME BASE AREA = Π
tan α = 1/2
l = Π tan α h/log h
Dw > Dc
Dw < Dc
4°.95
6°.98
7°.74
8°.4
9°.9
10°.3
NOSE HEIGHT H
WEDGE LENGTH L
0
2
4
6
8
10
12
14
16
18
20

Fig. 19

The results for l and h are plotted in Figure 19. This and other information is tabulated below.

TABLE

h	l	Width of wedge base	Wedge Angle
1			
1.5	5.81	.540	10.3
2.0	4.52	.695	9.9
2.5	4.26	.735	8.4
2.72	4.26	.735	7.74
3.0	4.26	.735	6.98
4.0	4.53	.692	4.95
5.0	4.87	.644	3.69
10.0	6.82	.460	1.32
20.0	10.5	.30	0.84

This indicates that the 'flying wing' type of supersonic craft may be of interest since a wedge of reasonable structural characteristics can be made to have less drag than a cone of the same height, especially in craft of larger size. Refinements of theory coupled with engineering considerations would probably give an optimum form somewhat different from the simple wedge here considered.

James B. Edson

James B. Edson

BIBLIOGRAPHY

1. Tracking Telescope Fundamentals - J. B. Edson
   Ballistic Research Laboratories Report #672
2. First Memorandum Report on the Jet Flame of the Flying A4 Missile - J. B. Edson.
   Optical Measurements Branch Report #1
3. Einfluss des Strahles auf die Aerodynamischen
   Eigenschaften des Aggregates A5
   Archives of Peenemunde, 12 March 1940
   Archive 66/23. German Document 631.23 in the Foreign Documents files of Aberdeen Proving Ground.
4. Widerstandsbeiwerte fur das A4VIP mit Beruckischtigung des Strahl - und Reibungseinfluses fur Unter und Uber schallgeschwindigkeiten - Untersuchung der Strahlexpansion.
   Archives of Peenemunde, 24 March 1943
   Archive 66/105 German Document GM10.111 in the Foreign Documents Files at Aberdeen Proving Ground
5. The Identification of Molecular Spectra
   R. Pearse and A. Gaydon.
6. Article in Physical Review, Vol. 42 (1932) Page 609
   P. C. Mahanti
7. Picatinny Arsenal Long Range Program
   Report on use of Sr. in Pyrotechnics
8. Handbook of Meteorology
   F. Berry, E. Ballay, and N. Beers, Editors
9. Pettit on Transmission of the Atmosphere
   Mt. Wilson Contrib. #445
10. Progress Reports, Project Hermes
    (Confidential)
11. Introduction to Theoretical Gas Dynamics
    Robert Sauer
12. Flame Temperature and Radiation Studies in Rockets.
    R. S. Craig. OSRD 5832 13044
13. Some Schlieren Photographs of Rocket Jets
    U. N. Mayall NDRC A332 9681
14. Supersonic Two-Dimensional Free Gas Jets
    D. C. Pack
15. Water Analogy to Two-Dimensional Air-Flow
    General Electric Research Laboratory 8/28/41

DISTRIBUTION LIST

No. of Copies	
6	ORDTB-Bal Sec
10	British (to ORDTB for distribution)
4	Chief, Bureau of Ordnance Navy Department Washington 25, D. C. Attn: Re3
1	Commanding Officer Naval Proving Ground Dahlgren, Virginia
2	Office of Naval Research Navy Department Washington 25, D. C. Attn: Scientific Literature Branch (N482) Parts "A", "C", and "DP" of GM/ML
1	Dr. R. W. Porter Project HERMES, General Electric Co. Schenectady, New York
1	Dr. H. J. Stewart, Jet Propulsion Lab. California Institute of Technology Pasadena, California
1	Dr. H. N. Russell Princeton University Princeton, N. J.
1	Dr. G. H. Dieke Johns Hopkins University Baltimore, Maryland
1	Dr. John Strong Johns Hopkins University Baltimore, Maryland
1	Dr. N. A. Christensen Dean of School of Engineering Cornell University Ithaca, New York

DEPARTMENT OF THE ARMY
UNITED STATES ARMY RESEARCH LABORATORY
ABERDEEN PROVING GROUND, MARYLAND 21005-5066

REPLY TO
THE ATTENTION OF

AMSRL-CS-IO-SC (380)

21 JUL 1999

MEMORANDUM FOR Defense Technical Information Center,
ATTN: DTIC-BCS, 8725 John J. Kingman Road
Suite 0944, Ft. Belvoir, VA 22060-6218

SUBJECT: Distribution Statement for Ballistic Research Laboratories Report No. 708

1. Reference: Ballistic Research Laboratories Report No. 708, "Optical Studies of the Jet Flame of the V-2 Missile in Flight", by J. B. Edson, October 1949, UNCLASSIFIED, AD number 801723.

2. Our Laboratory has determined that the referenced report may be released to the public. Request that you mark your copy of the document with the following distribution statement:

Approved for public release; distribution is unlimited.

3. Our action officer is Mr. Douglas J. Kingsley, telephone 410-278-6960.

Constance L. Berry
CONSTANCE L. BERRY
Acting Chief, Security/CI Office
ARL, APG